A COMPUTER MODEL STUDY OF UNSATURATED FLOW IN A LEACH DUMP

by

Rudolph H. Jacobson, Jr.

Submitted to the faculty of the
NEW MEXICO INSTITUTE OF MINING AND TECHNOLOGY
in partial fulfillment
of the requirements for the degree of
Doctor of Philosophy in Geoscience
July 1971

Table of Contents

ABSTRACT

A computer model was developed for the study of the flow of water or leaching solution through a leach dump. A two-dimensional, nonlinear, finite difference equation for an unsaturated porous medium was used for modeling fluid seeping from a source, such as a leach pond or a sprinkling system, into a vertical cross section of a layered leach dump.

Three cases of model leach dump profiles were run on a digital computer, showing the movement of fluid through both homogeneous and layered systems. The results of the cases run with the model will help to gain an understanding of the process of fluid flow in a leach dump as well as assist in the interpretation of data from such operations.

Acknowledgments

The author expresses his sincere graditude to Dr. Ronald J. Roman, Dr. Gerardo W. Gross, Dr. Willem F. Brutsaert, Dr. Ralph M. McGehee, and Mr. Merle E. Hanson, for their guidance and counsel as research advisors, and for their critical review of the manuscript. The advise, guidance and counsel of Dr. Roshan B. Bhappu was greatly appreciated.

The auther is also indebted to Mr. J. Rosenbaum and W. A. McKinny of the United States Bureau of Mines, Salt Lake City Metallurgical Research Center for providing the Research Fellowship which financed most of this study. Also, I am indebted to Dr. Marvin H. Wilkening, Dr. Gale K. Billings and Mr. Alvin J. Thompson for providing additional funds and guidance in support of this work.

The author is greatly indebted to my very good friends and colleagues, Chester McKee and Donald Beaver who entered into many interesting discussions of this work.

The author wishes to acknowledge the guidance and counsel of the late Professor Charles E. Jacob who helped initiate the direction of this study.

Finally, the author wishes to express his deepest appreciation to his wife and family for their constant support, encouragement and understanding during the course of this work.

List of Figures

List of Symbols

	Dimensions
$E = -dS_w/d\varphi_c$	L^{-1}
g = Acceleration of gravity	LT^{-2}
k = Absolute or intrinsic permeability	L^2
K = Saturated hydraulic conductivity	LT^{-1}
K_w = Hydraulic conductivity as a function of liquid saturation	LT^{-1}
$K_{w_{av}}$ = Average hydraulic conductivity as a function of liquid saturation, and defined between two adjacent grid cells	LT^{-1}
ℓ = a constant of the analytical solution	L^{-1}
L = Maximum horizontal length of flow domain of analytical solution	L
P_b = Bubbling pressure head	L
P_c = Capillary pressure head	L
P_w = Hydrostatic pressure, water or leach solution	$ML^{-1}T^{-2}$
Q_w = Source or sink term	T^{-1}
S_e = Effective saturation	-
S_{ri} = Irreducible liquid saturation	-
S_w = Liquid saturation, water or leach solution	-
t = Time	T
x = Horizontal distance	L
z = Vertical distance, for the leach dump problem z is positive downward	L
α, β = Constants of the effective saturation equations	-

σ = A dummy integration variable used in the analytical solution	-
Δ = Dimensions of a grid cell	L
Θ = An integration summation symbol used in the analytical solution	L
π = Pi (3.14)	-
μ = Viscosity of liquid	$ML^{-1}T^{-1}$
ρ_w = Density of liquid, water or leach solution	ML^{-3}
φ_c = Capillary potential head	L
φ_w = Liquid potential head, water or leach solution	L
ϕ = Porosity	-

INTRODUCTION

The Leach Dump

The leaching of waste ore dumps is the major method of secondary recovery of copper. In 1970, twenty percent of all domestic copper was produced by leach dump operations (Ballard, 1971).

A copper leach dump is normally composed of material assaying less than 0.4 percent copper. This waste rock is limited in size only by the capacity of the shovels and trucks that dig and haul the material from the open pit mines.

Sheffer and Evans (1968) indicate that most dumps in the United States range from 50 to 1200 feet high and cover a surface area from 100 to 1000 acres.

Howard (1968) found when bore-hole logging a leach dump that a distinct system of layers were present.

The leach solution added to the dump is mostly spent lixiviant from a precipitation plant. Additional water is always needed to make up for evaporation and other losses. The quantity of lixiviant varies from 1000 to 12,000 gallons per minute, depending on the size of the dump. This leach solution is added to the dump by spreading ponds and/or sprinkler systems. The ponds resemble long parallel ditches, 50 to 75

feet wide, 3 to 8 feet deep, with small earthen dams sectioning the ditch every 50 to 75 feet. The leach solution is held in a pond for several weeks at a depth of about five feet. After this wetting period, the usual practice is to fill ponds in a new area, bulldoze and rip the old dried out ponds, and completely rebuild them (Anon, 1966).

Over a period of years, a leach dump will settle and consolidate. This process of consolidation eventually reduces the fluid flow through the dump to such an extent that the overall leach operation is no longer profitable.

A complete study of the phenomenology of a leach dump requires knowledge of the simultaneous interaction of (1) the flow of leach solution, (2) the leaching process, and (3) the consolidation process.

Purpose

The purpose of this dissertation is to study the movement of water or leach solution through a model leach dump, using a numerical solution of a diffusion type of flow equation for approximating flow in an unsaturated porous medium.

Previous Work

Computer Models of Leach Dumps:

There has been very little work with computer models of fluid flow in the mining industry. Ballard (1971) in his review of the technical and theoretical advances made in the field of solution mining, does not mention the application of any fluid flow models to the study of leach dumps. However, Kealy and Williams (1970) describe a computer model study of fluid flow through a tailings pond dam. They used a steady state, finite element model.

In a recent AIME publication edited by A. Weiss (1969), A Decade of Digital Computing in the Mineral Industry, no mention is made of computer models to simulate fluid flow for analysis of problems of leach dumps, solution mining or groundwater flow in general.

Computer Models of Unsaturated Flow in Soil Physics:

In a very recent paper by Freeze (April, 1971) he describes a three-dimensional, transient, unsaturated flow model which can be used to study large scale water basins. Jeppson (1970) presented a detailed report on his development of a two-dimensional, transient, unsaturated flow model which was used to study the infiltration process.

In 1969 Freeze reviewed the state of the art of numerical models of flow in an unsaturated porous

medium, as pertains to soil physics. He lists fourteen publications pertaining to one-dimensional fluid flow models. Freeze's model is the only one listed which attempts to treat the dynamic water table. Rubin (1968) briefly outlines the basic theoretical concepts of his two-dimensional, transient, unsaturated flow model. He employed the alternating direction, implicit method to solve his set of finite difference equations.

Computer Models of Immiscible Flow in Reservoir Engineering:

Breitenbach, Thurnau and Van Poolen (1968a,b,c,d) presented a series of papers on the theoretical development of the fundamental flow equations for the simultaneous flow of oil, gas and water. They also describe some of the programming complications involved in developing computer models of multi-phase fluid flow.

Coats, Nielson, Terhune and Weber (1967) briefly outline a three-dimensional, two-phase computer model for the simultaneous flow of gas and oil. They described their method for incorporating into their model the relationship between capillary pressure and fluid saturation. They also presented a method for using a two-dimensional model to simulate certain types of three-dimensional problems.

An interesting publication by von Rosenberg (1969)

reviews the general principles and presents many solution schemes for the development of numerical models of mass transport and fluid flow.

Leach Dumps:

At the annual AIME meeting in Febuary, 1970, a short course on bioextractive mining was presented by E. Malouf of the Kennecott Copper Corporation. The course presented a detailed review of chemolithotrophic bacteria and their role in the dissolution of copper sulfides found in leach dumps. Bhappu, et al, (1969) presented a paper summarizing work on the complex iron salts present in the water flowing through a copper sulfide leach dump. They also discovered that most of the chemolithotrophic bacteria which produced these salts are located within the top ten feet of a leach dump. Since these bacteria need oxygen and carbon dioxide, the complete saturation of the top ten feet of a leach dump would probably inhibit their growth.

Harris (1969) discussed a method to examine the overall rate of copper sulfide dissolution for a leach dump. He developed a rate equation for application to this type of dump. Sheffer and Evans (1968) reviewed the copper leach dump operations in the Western United States. They summarized the operating methods and dump characteristics for seventeen different operations

in a detailed table for easy comparison.

The use of nuclear logging devices to locate dry, unleached areas within a leach dump was first reported on by Howard (1968). Woodcock (1967) presented an excellent review of leach dump construction and operation. He discussed in detail the leaching chemistry for copper sulfide dissolution and the precipitation of copper from the leach solution.

THEORETICAL CONSIDERATIONS

Mathematical Formulation

For soil-water flow systems in which the water replaces air or vice versa, it is often possible to ignore the flow of the air. This procedure may be acceptable because of the relatively small resistance to the flow of air since its viscosity is much less than the viscosity of the water or leach solution. In such cases it may be possible to consider the pressure of the air to be everywhere a constant, equal to the atmospheric pressure.

L. A. Richards (1931) developed a method for treating the fluid flow in an unconfined, unsaturated porous medium, whereby one equation of flow for the liquid phase is used to approximate the flow of air and water through a porous medium. He assumed that the atmospheric pressure p_a was a constant everywhere in the medium. Furthermore, assuming the liquid phase to be incompressible, a diffusion type of equation of the following form for two-dimensional vertical flow can be written as

$$\partial/\partial x(K_w \partial \varphi_c/\partial x) + \partial/\partial z(K_w \partial \varphi_c/\partial z) = -\phi\, \partial S_w/\partial t + Q_w \qquad 1$$

where

z, vertical distance measured positive downward in cm;

x, horizontal distance in cm;

t, time in sec;

K_w, hydraulic conductivity in cm/sec;

$\emptyset$, porosity;

φ_c, capillary potential head in cm, $\varphi_c = \varphi_w = -p_w/\rho_w g + z = p_c/\rho_w g + z$;

ρ_w, liquid density, usually water or leach solution in gm/cm^3;

g, acceleration due to gravity in cm/sec^2;

S_w, water saturation.

Q_w, source or sink term in sec^{-1}.

Equation 1 is the basic flow equation used in this study.

Functional Relationships

The hydraulic conductivity K_w, in equation 1 is a function of the amount of water or leach solution present in an unsaturated porous medium. An approximation for K_w as a function of the effective saturation S_e suggested in the literature (see Brooks and Corey, 1964) and used in this computer model is

$$K_w = K S_e^n \qquad 2$$

where

K, Saturated hydraulic conductivity in cm/sec;

S_e, effective saturation;

n, a constant, usually ranging from 2 to 4.

Because the computer model was computationally faster with n equal to 2, this value was used for all cases run in this study.

The effective saturation can be written

$$S_e = (S_w - S_{ri})/(1 - S_{ri}) \qquad 3$$

where S_{ri} is the irreducible water saturation.

McKee and Jacobson (paper in preparation) formulated two heuristic relationships for representing a curve of experimential data of capillary pressure head as a function of effective saturation. The first set of equations are

$$S_e = \exp(Arg1) \qquad \text{for } P_c > P_b \qquad 4$$

$$S_e = 1.0 \qquad \text{for } P_c \leq P_b \qquad 5$$

where

$$Arg1 = (P_b - P_c)/\beta P_b \qquad 6$$

and P_c, capillary pressure head in cm;

P_b, air entry or bubble pressure head in cm, (see Brooks and Corey, 1964);

β, a constant which can be varied to curve-fit an actual P_c versus S_e plot.

For equation 6, β usually ranges from 1.0 to about 2.0. Figure 1 shows a curve of actual data (Liakopoulas, 1963) approximated by equation 4. For this fit β was 1.2.

In order to better fit actual experimental data from about S_e equal to 0.8 to 1.0, a second equation, which is an extension of 4, is written as

$$S_e = 1/(1+\exp(Arg2)) \qquad 7$$

where

$$Arg2 = (P_c - \alpha P_b)/\beta P_b \qquad 8$$

For equation 8, the α and β constants used to approximate the real data of Figure 1 were 1.56 and 0.4 respectively.

The computer model used in this study requires the derivative of equation 7 with regard to S_w, as expressed by equation 3. This derivative,

$$dS_w/dP_c = -(1-S_{ri})\exp(Arg2)/(\beta P_b(1+\exp(Arg2))^2) \qquad 9$$

is continuous, always negative, and single-valued for all values of P_c, negative or positive in sign, on the curve generated by equation 7. In going through a

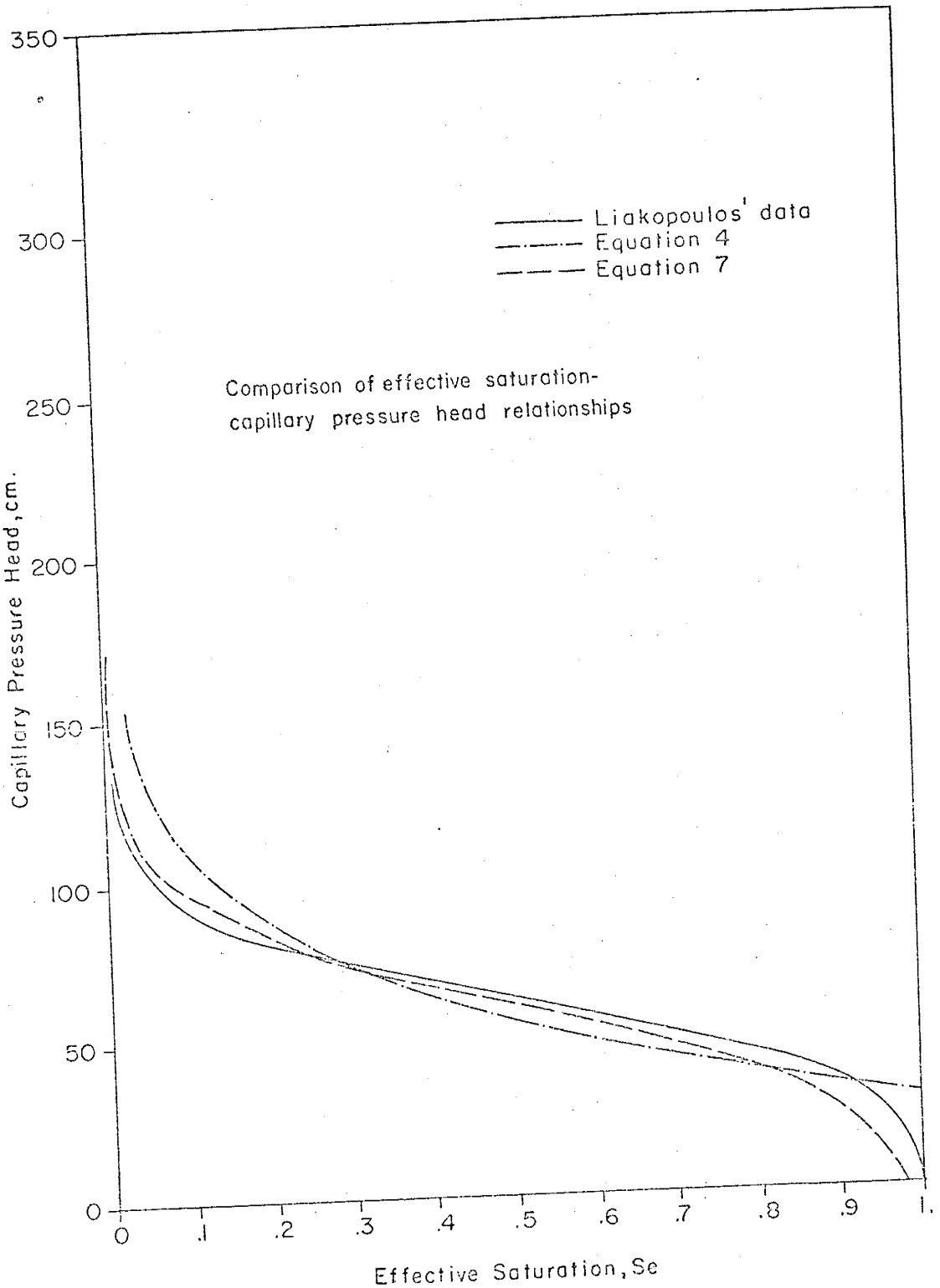
Liakopoulos' data
Equation 4
Equation 7
Comparison of effective saturation-
capillary pressure head relationships
Capillary Pressure Head, cm.
350
300
250
200
150
100
50
0
0
.1
.2
.3
.4
.5
.6
.7
.8
.9
1.
Effective Saturation, Se

Figure 1

water table the pressure heads change sign, but equation 9 remains negative.

The importance of equations 4 and 5 to this study are that they allow the development of a simple, transient analytical check solution of the computer model. The development of the analytical check solution is cover in the subsection Quantitative Verification-Analytical Check Solution.

The limitations of equations 2 and 7 to represent accurately different soil types under various flow conditions is covered more thoroughly in the subsection Model Limitations.

THE COMPUTER MODEL

Finite Difference Equation

The computer model is developed from a finite difference approximation of equation 1, written

$$\partial/\partial x(K_w \partial \varphi_c/\partial x) + \partial/\partial z(K_w \partial \varphi_c/\partial z) = -\phi\, \partial S_w/\partial t + Q_w \qquad 1$$

The time derivative of the above equation can be expanded as

$$-\partial S_w/\partial t = - dS_w/dP_c\, \partial P_c/\partial t \qquad 10$$

since S_w is assumed a function of P_c only. Furthermore,

$$P_c = \varphi_c - z \qquad 11$$

or

$$\partial P_c/\partial t = \partial \varphi_c/\partial t \qquad 12$$

resulting in 10 being written as

$$-\partial S_w/\partial t = - dS_w/dP_c\, \partial \varphi_c/\partial t \qquad 13$$

In equation 13 dS_w/dP_c is set equal to equation 9. For simplicity $-dS_w/dP_c$ is designated E. We can now write equation 1 as

$$\partial/\partial x(K_w \partial \varphi_c/\partial x) + \partial/\partial z(K_w \partial \varphi_c/\partial z) = \phi E \partial \varphi_c/\partial t + Q_w \qquad 14$$

Equation 14 is expressed in the fully implicit finite difference form as

$$1/\Delta x^2 (K^{n+1}_{W_{i+\frac{1}{2},j}} (\varphi^{n+1}_{c_{i+1,j}} - \varphi^{n+1}_{c_{ij}}) - K^{n+1}_{W_{i-\frac{1}{2},j}} (\varphi^{n+1}_{c_{ij}} - \varphi^{n+1}_{c_{i-1,j}})) +$$

$$1/\Delta z^2 (K^{n+1}_{W_{i,j+\frac{1}{2}}} (\varphi^{n+1}_{c_{i,j+1}} - \varphi^{n+1}_{c_{ij}}) - K^{n+1}_{W_{i,j-\frac{1}{2}}} (\varphi^{n+1}_{c_{ij}} - \varphi^{n+1}_{c_{i,j-1}}))$$

$$= \phi_{ij} E^{n+1}_{ij} (\varphi^{n+1}_{c_{ij}} - \varphi^{n}_{c_{ij}})/\Delta t^{n+\frac{1}{2}} + Q_{W_{ij}} \qquad 15$$

In this computer model Δx is equal to Δz thus each grid cell of the model domain has equal dimensions in the x and z directions. The superscripts $n+1$ refer to a new position on the time or temporal grid system. The subscripts refer to a position in space. For example, $i+\frac{1}{2},j$ is located on the midpoint of the right hand side of the ith spatial grid cell as shown in Figure 2.

Setting $\Delta x = \Delta z = \Delta$ and expanding equation 15 results in

$$-\varphi^{n+1}_{c_{ij}} (K^{n+1}_{W_{i+\frac{1}{2},j}} + K^{n+1}_{W_{i-\frac{1}{2},j}} + K^{n+1}_{W_{i,j+\frac{1}{2}}} + K^{n+1}_{W_{i,j-\frac{1}{2}}}) + K^{n+1}_{W_{i,j-\frac{1}{2}}} \varphi^{n+1}_{c_{i,j+1}}$$

$$+ K^{n+1}_{W_{i,j-\frac{1}{2}}} \varphi^{n+1}_{c_{i,j-1}} - \Delta^2 \phi_{ij} E^{n+1}_{ij} \varphi^{n+1}_{c_{ij}}/\Delta t^{n+\frac{1}{2}} =$$

$$- K^{n+1}_{W_{i+\frac{1}{2},j}} \varphi^{n+1}_{c_{i+1,j}} - K^{n+1}_{W_{i-\frac{1}{2},j}} \varphi^{n+1}_{c_{(-1,j}} - \Delta^2 \phi_{ij} E^{n+1}_{ij} \varphi^{n}_{c_{ij}}/\Delta t^{n+\frac{1}{2}}$$

$$+ \Delta^2 Q_{W_{ij}} \qquad 16$$

Equation 16 is reduced to the following simplified form,

$$\varphi^{n+1}_{c_{i,j-1}} A_j + \varphi^{n+1}_{c_{ij}} B_j + \varphi^{n+1}_{c_{i,j+1}} C_j = D_j \qquad 17$$

where

$$A_j = K^{n+1}_{W_{i,j-\frac{1}{2}}} \qquad 18$$

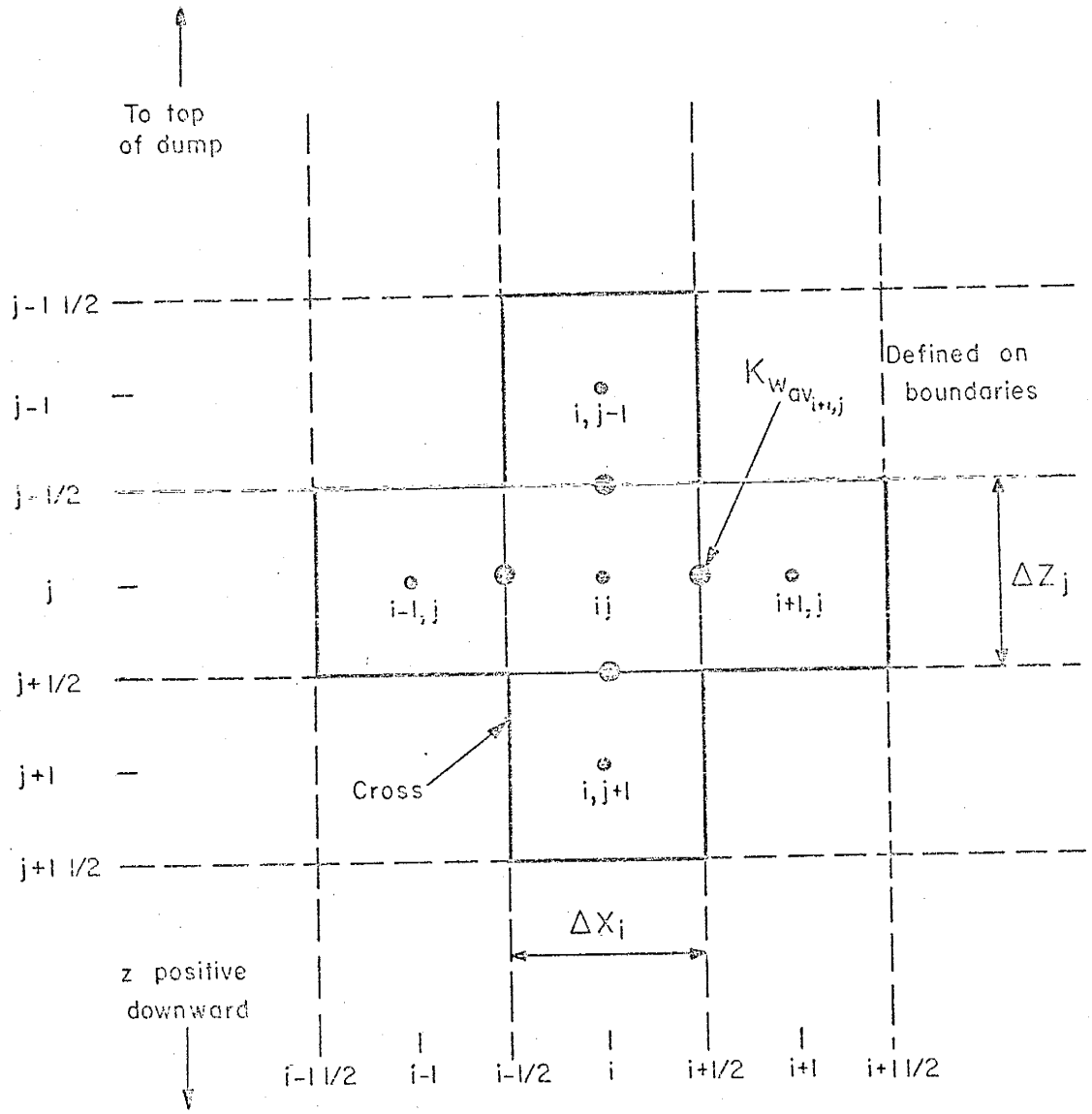

Computer grid representation

Figure 2

$$B_j = -\left(K_{W_{i+\frac{1}{2},j}}^{n+1} + K_{W_{i-\frac{1}{2},j}}^{n+1} + K_{W_{i,j+\frac{1}{2}}}^{n+1} + K_{W_{i,j-\frac{1}{2}}}^{n+1} + \Delta^2 \phi_{ij} E_{ij}^{n+1} / \Delta t^{n+\frac{1}{2}}\right) \quad 19$$

$$C_j = K_{W_{i,j+\frac{1}{2}}}^{n+1} \quad 20$$

$$D_j = -\left(\Delta^2 \phi_{ij} E_{ij}^{n+1} \varphi_{c_{ij}}^{n} / \Delta t^{n+\frac{1}{2}} + \varphi_{c_{i+1,j}}^{n+1} K_{W_{i+\frac{1}{2},j}}^{n+1} + \varphi_{c_{i-1,j}}^{n+1} K_{W_{i-\frac{1}{2},j}}^{n+1}\right) + \Delta^2 Q_{W_{ij}} \quad 21$$

Equation 17 is solved in every grid cell simultaneously within each row or column of the flow domain using a matrix solution technique adapted for digital computers, the Thomas algorithm (see Appendix A). This rountine is often referred to as a line, or block, Gauss-Seidel (see Ames, 1965), since a row or column of grid cells is solved at a time. Equation 17 is written such that the grid cells within a column are solved by a vertical sweep, going from top to bottom, and left to right. A horizontal sweep procedure is developed in Appendix B for solving the grid cells a row at a time time, going from left to right, and top to bottom. The computer program is written to solve the flow domain by alternating between solving rows then columns for successive iterations of each time step.

In equation 16 the K_W's and E are superscripted $n+1$. This means that they are updated each iteration of every time step, thus being solved at the new time step. The K_W's are subscripted, for example $K_{W_{i+\frac{1}{2},j}}$. Figure 2 shows that $K_{W_{i+\frac{1}{2},j}}$ is centered between the i,j and the $i+1,j$ grid cells. Appendix E explains in detail

the method developed for this computer model for averaging the K_w's on the grid cell boundaries.

Computational Scheme

The following is an outline of the order in which calculations are made for one time step. Figure 3 is a flow diagram illustrating the steps taken to calculate a solution.

Step 1. Initialization

Read in liquid properties and the initial hydrologic properties for each grid cell within the flow domain. Calculate within each grid cell the following:

$$P_c = \alpha P_b + \beta P_b \ln(1/S_e - 1) \quad \text{(from equation 7)} \qquad 22$$

$$\varphi_c^n = P_c + z \qquad 11$$

$$K = k\rho_w g/\mu \qquad 23$$

where

k = intrinsic or absolute permeability in darcys;

μ = liquid viscosity in dyne-sec/cm^2;

$\varphi_c^{n+1} = \varphi_c^n$

The first time step size is read in, usually one second.

Step 2. Determination of a new time step size

Essentially the old time step size is increased by some predetermined amount, for example, a 10% increase. Appendix C has a more detailed description of this routine.

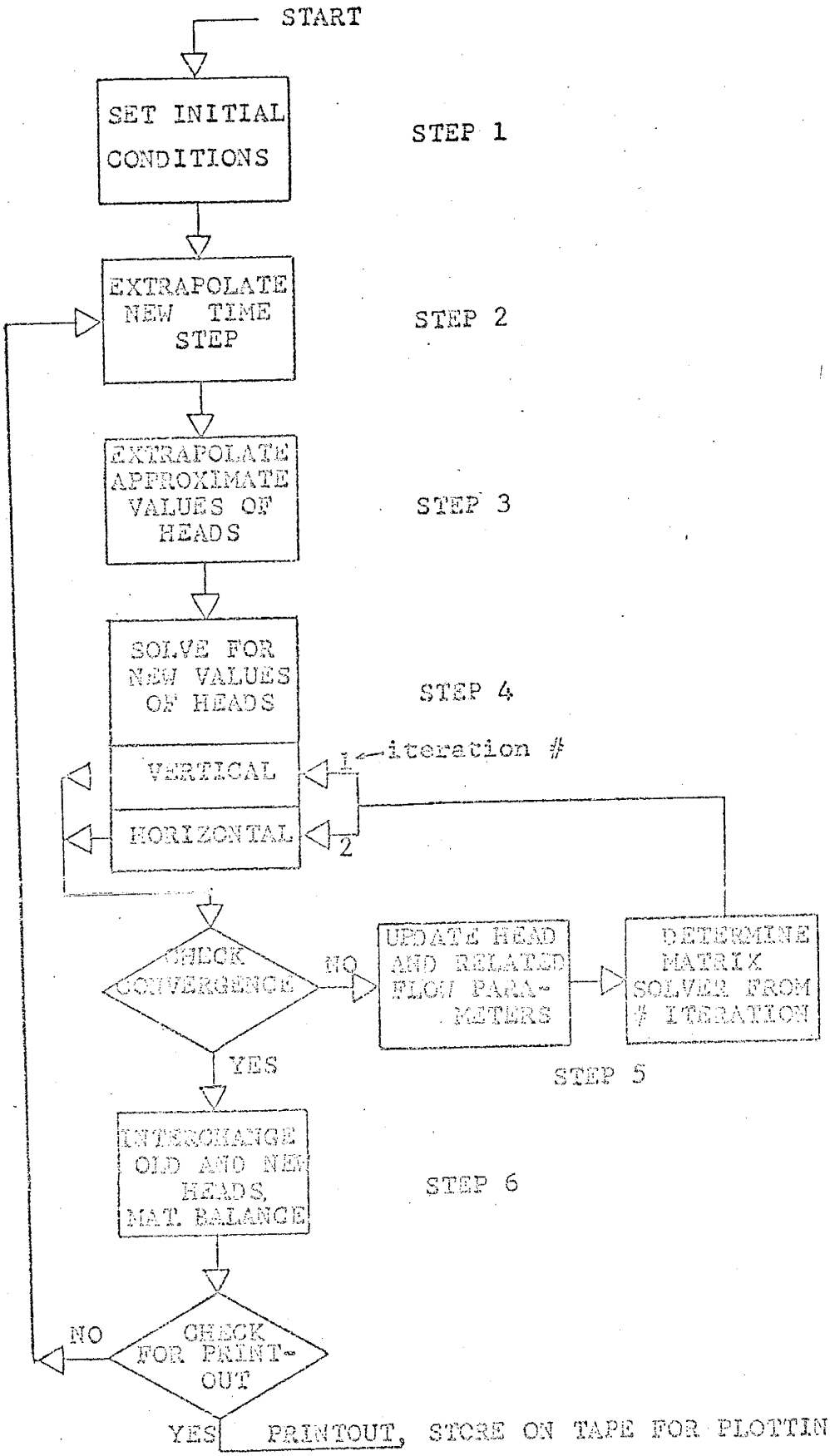

FIGURE 3 Computer flow diagram

Step 3. Extrapolate new capillary pressure heads

Extrapolate new, approximate values for the dependent variables, φ_c. The rate of change of φ_c is approximated by

$$\Delta\varphi_c(\text{old})/\Delta t(\text{old}) = \Delta\varphi_c(\text{new})/\Delta t(\text{new}) \qquad 24$$

Solving for $\Delta\varphi_c(\text{new})$ gives

$$\Delta\varphi_c(\text{new}) = (\Delta t(\text{new})/\Delta t(\text{old}))\Delta\varphi_c(\text{old}) \qquad 25$$

The exact formulation is presented in Appendix D.

From these approximate φ_c's, new values of the hydrologic properties are calculated as,

$$P_c = \varphi_c(\text{new}) - z \qquad 26$$

$$\text{Arg2} = (P_c - \alpha P_b)/\beta P_b \qquad 8$$

$$E = (1-S_{ri})\exp(\text{Arg2})/(\beta P_b(1+\exp(\text{Arg2})^2) \qquad 27$$

$$S_e = 1/(1+\exp(\text{Arg2})) \qquad 7$$

Step 4. Solving for new values of capillary pressure head

Equation 17 is solved in every grid cell of the flow domain. Also, the average values of the hydraulic conductivities are calculated on the boundaries between grid cells. Appendix E has a detailed description of this formulation.

The new values of φ_c are checked for convergence. If all the new φ_c's pass the convergence test, proceed to step 6, where the new φ_c's are interchanged with the old φ_c's of the preceeding time step. Also, from

these new values of φ_c, there corresponding values of S_w, P_c and K_w are calculated and printed out.

If the convergence test was not passed, proceed to Step 5, where the values of P_c and S_e are updated from the most recent values of φ_c. Proceed back to Step 4, update the iteration counter to 2, and calculate new values of φ_c everywhere within the flow domain. For odd numbered iterations the matrix is solved by columns. For even numbered iterations the matrix is solved by rows. Solving the matrix, first by columns then by row (or vise versa) for successive iterations reduces the numberof iterations to converge significantly.

For this computer model the boundary conditions are designated in Step 1, by setting all of the absolute conductivities in the boundary grids equal to zero. From Appendix E, equation (E-2), we see that these zero absolute conductivities results in zero average hydraulic conductivities at the boundary grid cells, thus producing a no-flow boundary.

Fluid flow into and out of the model flow domain is accomplished with the source terms, which approximate a constant flux condition.

Testing of the Computer Model

Model Limitations:

The computer model used in this study and presented in Appendix I has the following limitations:

1. The model will not simulate the drainage-imbibition hysteresis effect between P_c and K_w or P_c and S_w.
2. The pore size distribution curve for the porous medium being simulated is assumed to have a normal bell-shaped distribution curve, without skew. The standard deviation for the pore size distribution curve is assumed to be constant. This limitation becomes evident since equation 9 is proportional to the pore size distribution (see Brutsaert, 1966). In order to fit a P_c-S_e curve perfectly with equation 7 the constant β (or the combination βP_b) must be varied according to the value of S_e. In all probability β or βP_b is directly proportional to the standard deviation of the pore size distribution curve. If β varies with S_e then the shape of the pore size distribution curve must be skewed.
3. For a smooth distribution of S_w and P_c within the flow domain a spatial stability criterion has been determined whereby the P_b (in cm) of a soil represented by a grid cell should not be <u>less</u> than the grid cell dimensions.
4. The <u>initial</u> liquid saturation represented by a grid cell can not be less than or equal to the S_{ri} of that

cell. This condition is due to the fact that equation 22, which calculates the initial P_c from the initial S_e, has S_e in the denominator. When S_w is equal to S_{ri} then S_e is zero, resulting in an infinite value for the initial P_c.

5. The value of n of equation (E-2) (see Appendix E) can not be easily varied for different soil types within the flow domain. It was found that to represent equation (E-2) in the model by the exponential method of raising S_e to a power, resulted in considerable roundoff error in the final solution. To overcome this difficulty it was necessary to raise the arithmetic average of the S_e's to the power of 2 by using the method of squaring the averages. Since this technique is permanently written into the computer program, one can not use other values of n without changing the present program.

6. Due to computer storage limitations the present model is limited to a flow domain of 22 by 22 grid cells. This limitation coupled with the fact that the grid sizes should be no greater than the P_b of the soil it represents, reduces the size of the model leach dump profiles to about 50 foot by 50 foot square.

7. The computer model uses only the static equilibrium P_c-S_w curve.

Qualitative Verification:

The validity of Richards' equation to approximate unconfined, unsaturated fluid flow in a porous medium has been firmly established, beginning with Richards (1931) who checked the results of experimental data with a one-dimensional analytical solution of his equation under the conditions of (1) constant air pressure, (2) incompressible liquid phase and (3) unconfined fluid flow in a porous medium.

Rubin (1968) developed a two-dimensional, transient numerical solution of Richards' equation, with which he obtained meaningful results for the case of infiltration and drainage of specific soil types.

Recently, Freeze (1971) developed a three-dimensional, transient computer model using a modification of Richards' equation, whereby he added terms to the equation to account for the compressibility of the fully saturated porous medium. He suggests that the model gives good results for natural saturated-unsaturated flow systems.

The following preliminary tests were made with the computer model developed in this study:

1. A capillary rise condition was simulated by introducing a constant head boundary condition (see Appendix H) at the bottom boundary into a homogeneous porous medium of constant initial liquid saturation slightly greater then the irreducible saturation.

2. The settling of liquid was modeled, starting with various initial saturations. These tests were run until the liquid virtually ceased to flow everywhere within the flow domain. At this time the distribution of liquid with height followed the P_c-S_w curve for the homogeneous type soils.

3. A check on the model to simulate a two-dimensional fluid flow condition was made by vertically dividing a 10 by 10 grid cell flow domain into two equal parts. The initial liquid saturation in one half of the flow domain was set slightly larger than the S_{rl}. The other half of the flow domain was set fully saturated. The model was run until all of the liquid in the fully saturated half of the flow domain was equally distributed throughout the whole domain.

In all of the tests the computer model conserved liquid to within 3 percent total cumulative error in the material balance (see Appendix F). The final results of each of these tests agreed with the physics of the problem.

A rough estimate was made of the convergence coefficient R (spectral radius). The value of R was found to be approximately 0.97. The value of the error is approximately

$$\text{error} \approx \left[R/(1-R)\right] \left| \varphi^{n+1} - \varphi^{n} \right|$$

The error is then of the order of

$$\left[R/(1-R)\right] \text{TOL} = 1.5 \times 10^{-3}$$

where TOL was the tolerance used in the computer model equal to 5×10^{-5}.

Quantitative Verification-Analytical check solution:

A one-dimensional analytical solution for horizontal flow out of a nearly saturated porous medium was developed to check the computer model flow behavior. This solution can only approximate the numerical solution since the computer model uses equation 7 to represent S_e as a function of P_c, whereas the analytical solution was developed using equation 4. Futhermore, the computer model is a two-dimensional solution, hence the results of the one-dimensional check problem can only suggest that the model may simulate correctly the fluid flow in two dimensions.

In one-dimension the partial differential equation for horizontal flow is

$$\partial/\partial x(K_w\, \partial\varphi_c/\partial x) = -\phi\, \partial S_w/\partial t \qquad 28$$

Since

$$\varphi_c = P_c + z \qquad 29$$

then

$$\partial\varphi_c/\partial x = \partial P_c/\partial x \qquad 30$$

resulting in

$$\partial/\partial x(K_w\, \partial P_c/\partial x) = -\phi\, \partial S_w/\partial t \qquad 31$$

With the integral transformation (see Carslaw and Jaeger, 1959, p. 89)

$$\theta = \int_{P_b}^{P_c} (K_w(\sigma)/K)d\sigma \qquad 32$$

where K_w is a function of P_c only then

$$K\,\partial\theta/\partial x = K_w\,\partial P_c/\partial x \qquad 33$$

$$K\,\partial\theta/\partial t = K_w\,\partial P_c/\partial t \qquad 34$$

Assuming S_w is a function of P_c only results in right hand side of equation 31 being written as

$$-\phi\,\partial S_w/\partial t = -\phi(dS_w/dP_c)\,\partial P_c/\partial t$$
$$= -\phi(K/K_w)\,(dS_w/dP_c)\,\partial\theta/\partial t \qquad 35$$

Substituting equations 30, 33, 34 and 35 into 28 results in

$$\partial(\partial\theta/\partial x)/\partial x = -\phi/K_w\,(dS_w/dP_c)\,\partial\theta/\partial t \qquad 36$$

From equation 3 and 4 dS_w/dP_c can be expressed as

$$dS_w/dP_c = -((1-S_{ri})/\beta P_b)\,\exp((P_b-P_c)/\beta P_b) \qquad 37$$

Assuming n equal to 1 in equation 2 results in

$$K_w = K\,\exp((P_b-P_c)/\beta P_b) \qquad 38$$

which reduces equation 36 to

$$\partial\theta^2/\partial x^2 = (\phi(1-S_{ri})/\beta P_b K)\,\partial\theta/\partial t \qquad 39$$

Integrating 32 results in

$$\theta = P_b\beta(1-\exp((P_b-P_c)/\beta P_b) \qquad 40$$

In equation 39 let

$$k = \phi\,(1-S_{ri})/\beta P_b \qquad 41$$

The solution for

$$P_c(x,o) = P_b \Rightarrow \theta(x,o) = 0$$

with boundary conditions

$$K_w \, \partial P_c/\partial x(o,t) = 0 \Rightarrow K \, \partial\theta/\partial x(o,t) = 0$$

and with the flux condition for <u>removal</u> of liquid from the flow domain as

$$K_w \, \partial P_c/\partial x(L,t) = - F_o = - K \, \partial\theta/\partial x = Q_w \Delta \qquad 42$$

The final solution in terms of θ is taken from Carslaw and Jaeger, (1959), p.112, and is written

$$\theta(x,t) = F_o t/\lambda L + (F_o L/K)((3x^2-L^2)/6L^2 - (2/\pi^2)\sum_{n=1}^{\infty}(-1)^n \frac{1}{n^2}\exp(A)\cos(B)) \qquad 43$$

where 44

$$A = (K/\lambda)n^2\pi^2 t/L^2 \qquad 45$$

$$B = n\pi x/L$$

L = maximum horizontal length of the flow domain

and 46

$$P_c = P_b - \beta P_b \ln(1-\theta/\beta P_b)$$

The sign convention used by Carslaw and Jaeger implies that $-F_o$ means liquid is being pumped out of the system.

Both the analytical and numerical soultions were run to remove water from a horizontal strip 20 grid cells long, each grid cell being 30 cm long, or L = 600 cm.

The initial hydrologic properties were;

ϕ = 30%

K = 0.0133 cm/sec

S_{wi} = 30%

S_w = 0.985 (model)

S_w = 1.0 (analytical)

P_c = zero (model)

P_c = 30 cm (analytical)

α = 1.56 (model)

β = 0.4 (model)

β = 1.2 (analytical)

Figure 1 shows the P_c-S_e curves followed by both the model and the analytical solutions. Note that the curve generated by equation 4, the same relationship used in the analytical solution, deviates from the curve generated by equation 7, the relationship used in the computer model, at both ends of the curves.

These two curves are fairly well matched over most of the range of S_e. Figure 4 shows that as a function of time and distance the model and the analytical solutions are in good agreement, where the curves of Figure 1 agree. The deviations of the curves of Figure 4 correspond to the deviations of the P_c-S_e curves of Figure 1. This check on the numerical solution, and the method used to average the hydraulic

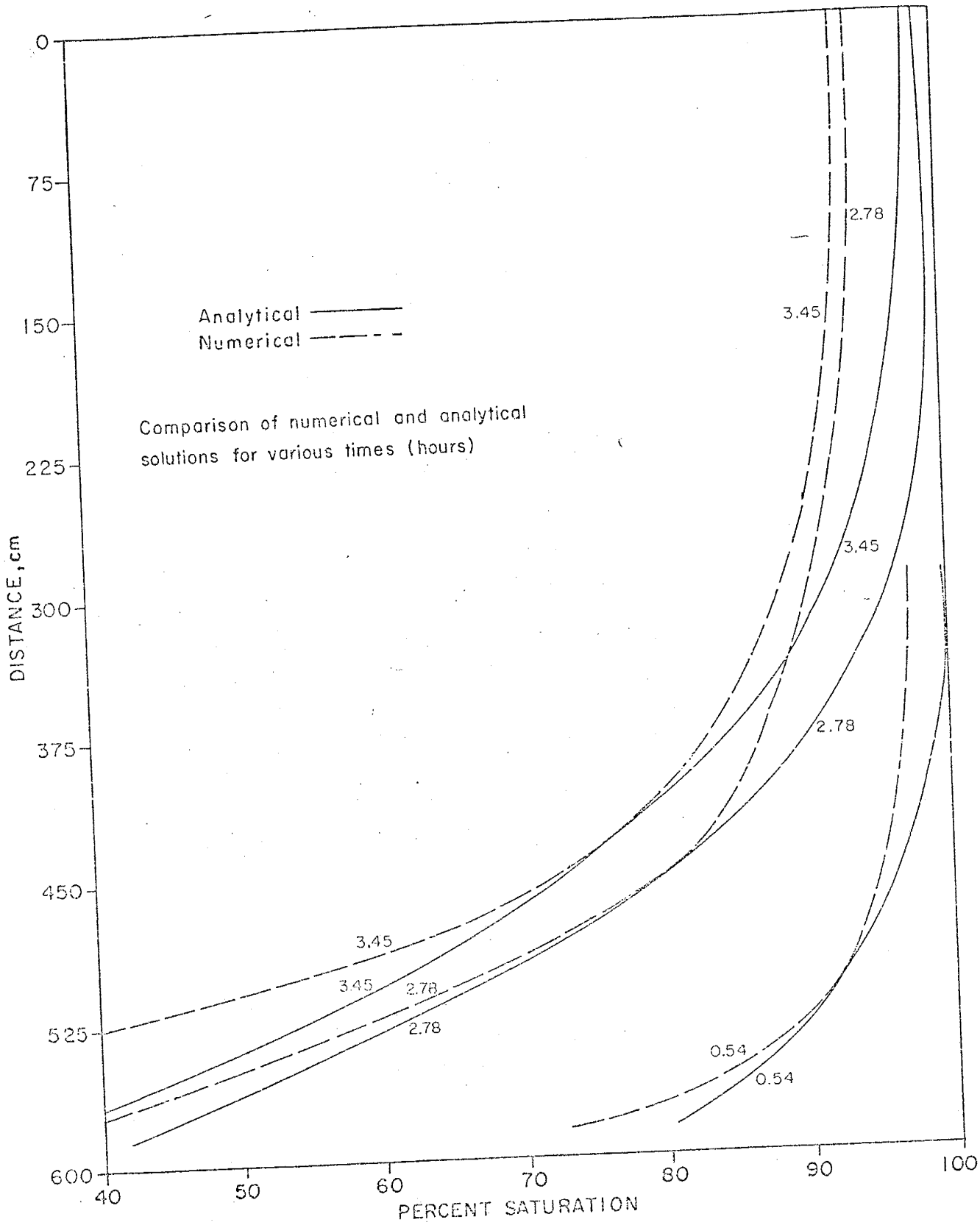
Analytical
Numerical
Comparison of numerical and analytical solutions for various times (hours)
DISTANCE, cm
PERCENT SATURATION
0
75
150
225
300
375
450
525
600
40
50
60
70
80
90
100
2.78
3.45
3.45
2.78
3.45
2.78
2.78
0.54
0.54

Figure 4

conductivities between grid cell broundaries is sufficient to establish that the computer model will satisfactorly approximate one-dimensional fluid flow in an unsaturated porous medium, such as a leach dump.

DISCUSSION OF RESULTS OF LEACH DUMP SIMULATION

Three examples of fluid flow in both homogeneous and layered unsaturated porous media were simulated with the computer model. In all three cases the source terms were arranged (dark strip at top, center of Figures 5 through 13) such as to show the edge of a leach pond 25 foot wide and 2.5 feet deep. Ten source terms were used in a row to inject at a constant rate of $1 \times 10^{-4} sec^{-1}$. All boundaries were no-flow. This in effect means that the model is in an impervious box, of dimensions X·Z·1cm.

To calculate the quantity of leach solution being injected in terms of gallons and square feet of ponded surface area, the following calculation was made;

$$\text{Rate}(gal/ft^2\text{-min}) = Q_w \cdot \Delta(ft) \cdot 60(sec/min) \cdot 7.48(gal/ft^3)$$

$$= 0.11\ gal/ft^2\text{-min}$$

This rate is higher than most injections rates found in actual practice, but about average for start-up in a newly bulldozed ponded area.

The fluid properties used in all three cases were,

liquid density = 1.1 gm/cm^3

liquid viscosity = 0.008 poises

and the time step size was limited to a maximum change of 10 percent. The φ_c's were held to no greater than 10 percent per time step. The α and β constants of

equations 7 and 9 were kept 1.56 and 0.4 respectively for all soil types modeled. The soil types used in the model are called fine sand, coarse sand, and clay for convienence in describing the cases.

Case 1 Homogeneous Fine Sand

Initial Hydrologic Properties:

S_w = 40 %

S_{ri} = 30 %

ϕ = 30 %

k = 10 darcys

P_b = 91.44 cm

Figures 5 through 7 represent the saturation profiles with flux vectors for the simulation of fluid flow over a period of 9.67 hours. In Figure 5 we see that after 2.54 hours the movement of the wetting front has progressed downward in a fan shaped pattern. Also some liquid has already started to settle in the bottom of the flow domain.

Figure 6 shows that after 8.26 hours the formation of a distinct water table, also the fan shaped pattern has disappeared. In computer contouring the saturation contours, all saturations greater than 98 % are included as part of the isopiestic line defining the dynamic water table. This line is the zero capillary pressure line. Due to the presence of an impermeable bottom boundary, the saturation contours are becoming

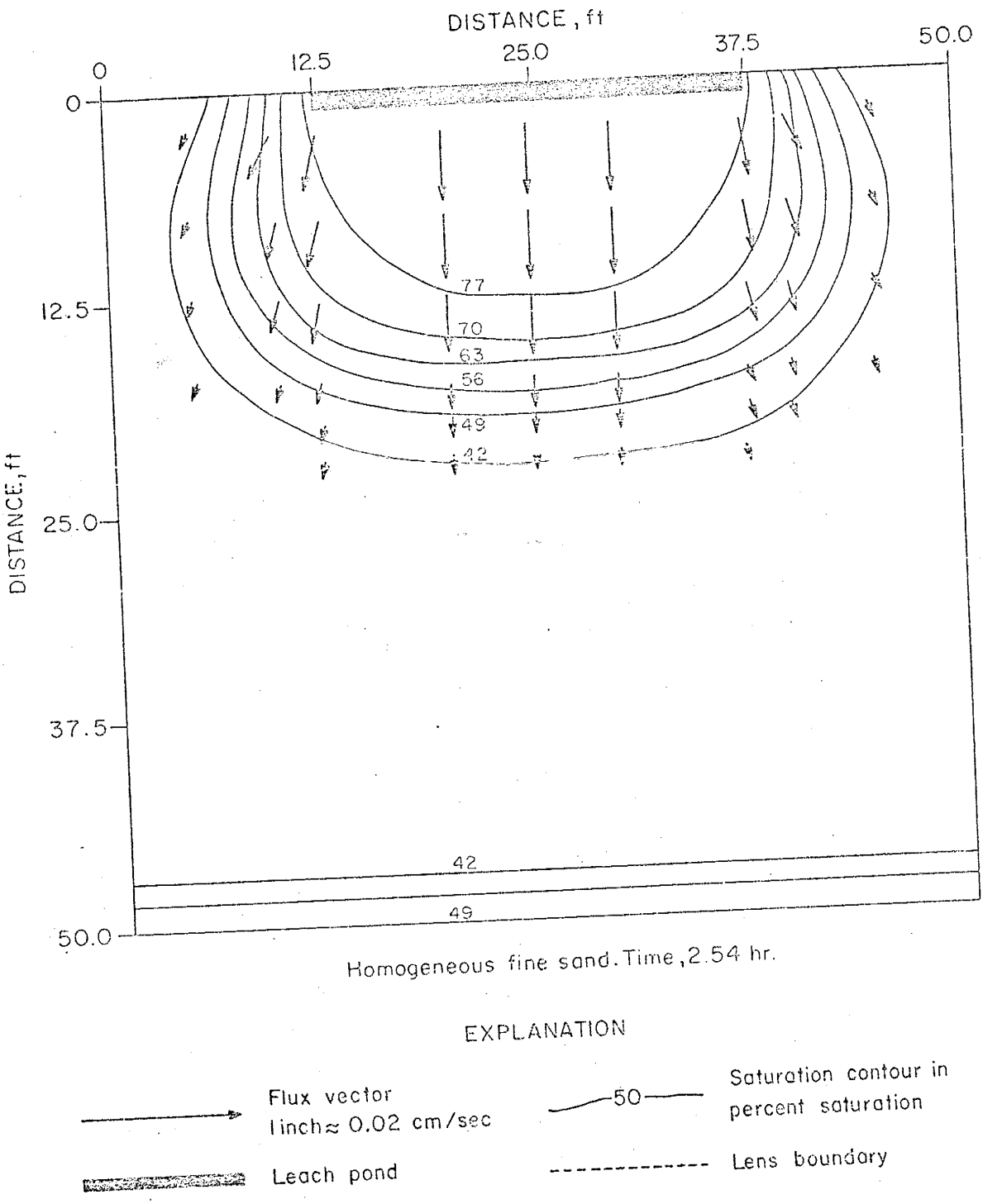
DISTANCE, ft
0
12.5
25.0
37.5
50.0
DISTANCE, ft
77
70
63
56
49
42
42
49
Homogeneous fine sand. Time, 2.54 hr.
EXPLANATION
Flux vector
1 inch ≈ 0.02 cm/sec
50
Saturation contour in percent saturation
Leach pond
Lens boundary

Figure 5

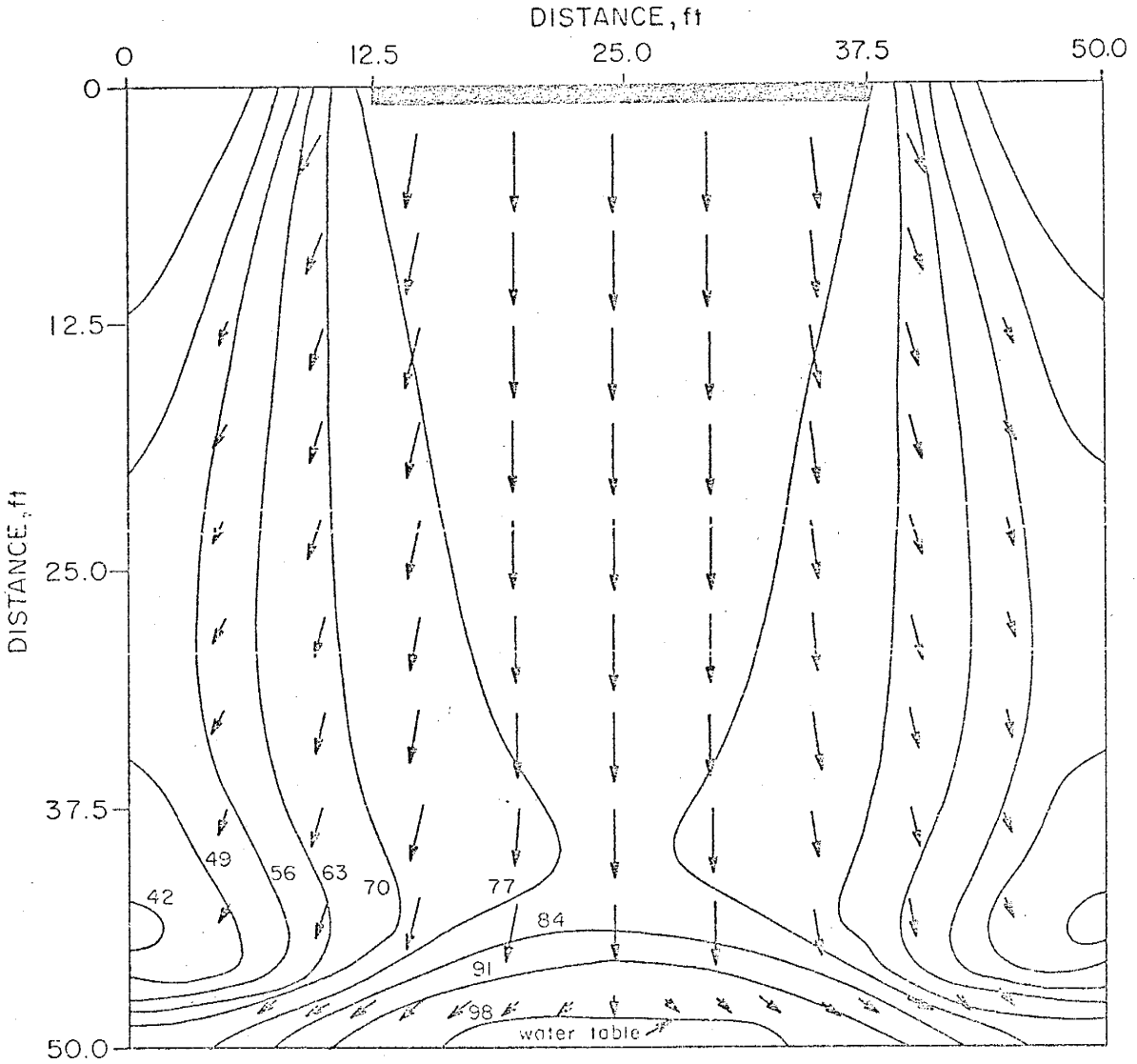

Homogeneous fine sand. Time, 8.26 hr.

EXPLANATION

Flux vector
1 inch ≈ 0.02 cm/sec

50 — Saturation contour in percent saturation

Leach pond

Lens boundary

Figure 6

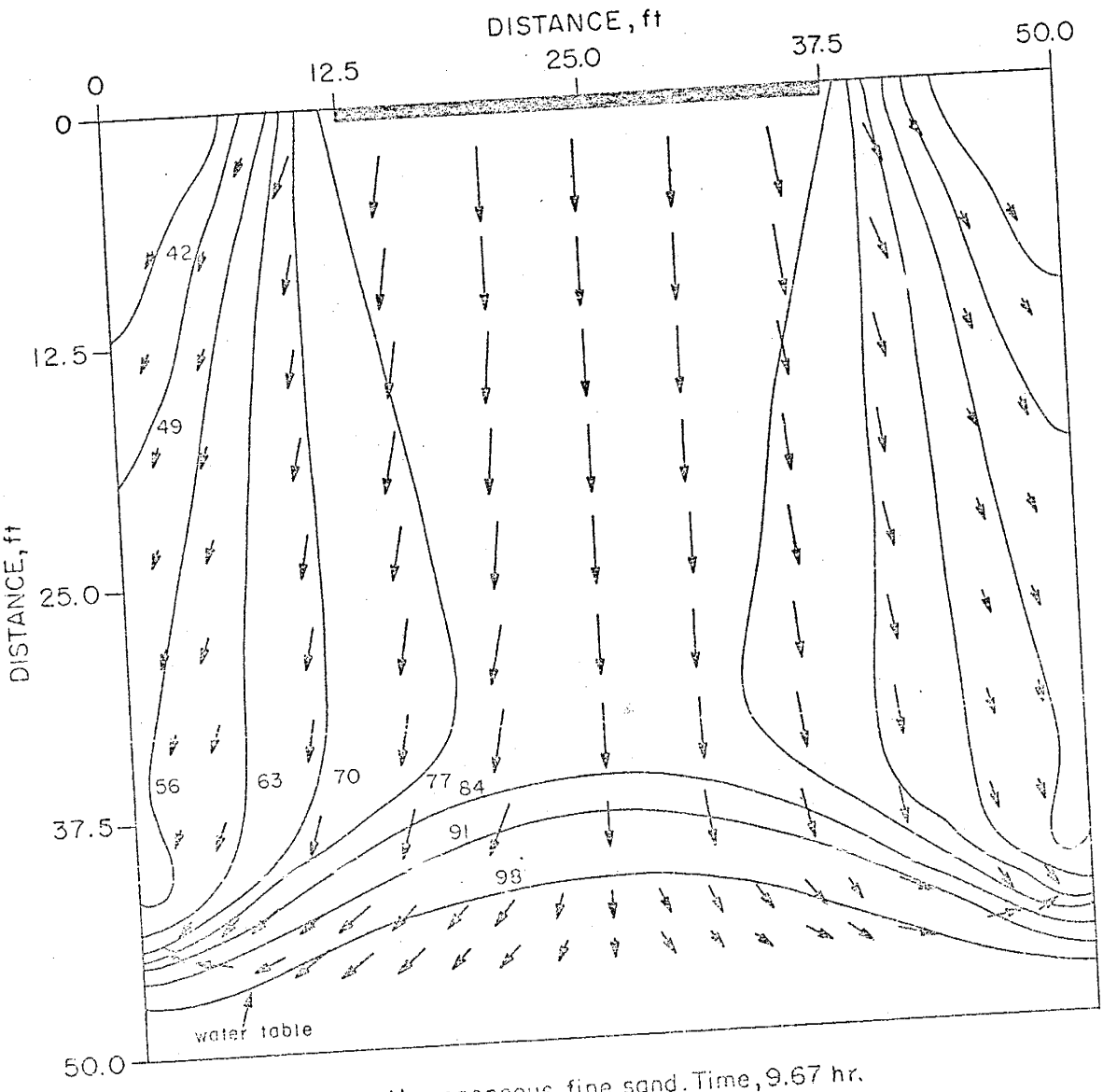

EXPLANATION

Flux vector
1 inch ≈ 0.02 cm/sec

50 — Saturation contour in percent saturation

Leach pond

Lens boundary

Figure 7

distorted. The length of the flux vectors in the center of Figure 6 indicates that the maximum flow velocity is directly beneath the center of the leach pond.

Figure 7 shows that after 9.67 hours the water table is rising as a gentle mound. The flux vectors are moving toward the drier regions on both sides of the flow domain.

The computing time to calculate the results of Figure 7 was approximately 30 minutes on an IBM, Model 44.

Case 2 Coarse Sand Lens in Fine Sand

Initial Hydrologic Properties:

A. Coarse Sand Lens

S_w = 40 %

S_{ri} = 30 %

ϕ = 50 %

k = 100 darcys

P_b = 76.2 cm

B. The fine sand surrounding the coarse sand lens is the same as in Case 1.

Figures 8 through 10 illustrate the effect that a coarse sand lens can have on the fluid flow pattern of Case 1. The lens, indicated by the dashed box, is

located in the center of the flow domain. This case was intended to show how the model could be made to simulate the channeling effect often observed in an actual leach dump. Whereas, the channeling effect may actually be flow of solution on a scale similar to flow in an open pipe or channel, on a large scale the effect can be simulated by a material of very large permeability. It is possible when attempting to model this situation to have the coarse sand lens, of small P_b, in a fine sand or clay of a very large P_b such that the water can be removed from the lens due to the very large difference in capillary pressure heads, before the arrival of the wetting front, whereby the hydraulic conductivity as a function of liquid saturation within the lens drops to such a small value in comparison to the surrounding medium that a perched water table will develop on top of the coarse sand lens until water has had time to re-saturate the coarse sand lens. Several cases were run to model this type of problem with very good results.

Figure 8 shows that the fluid flow tends to channel through the coarse sand lens. The fluid flow through the lens is fast enough, compared to flow in the surrounding medium, that the average saturation is small compared to the values just outside of the lens.

Figure 9 shows that after 7.21 hours a distinct

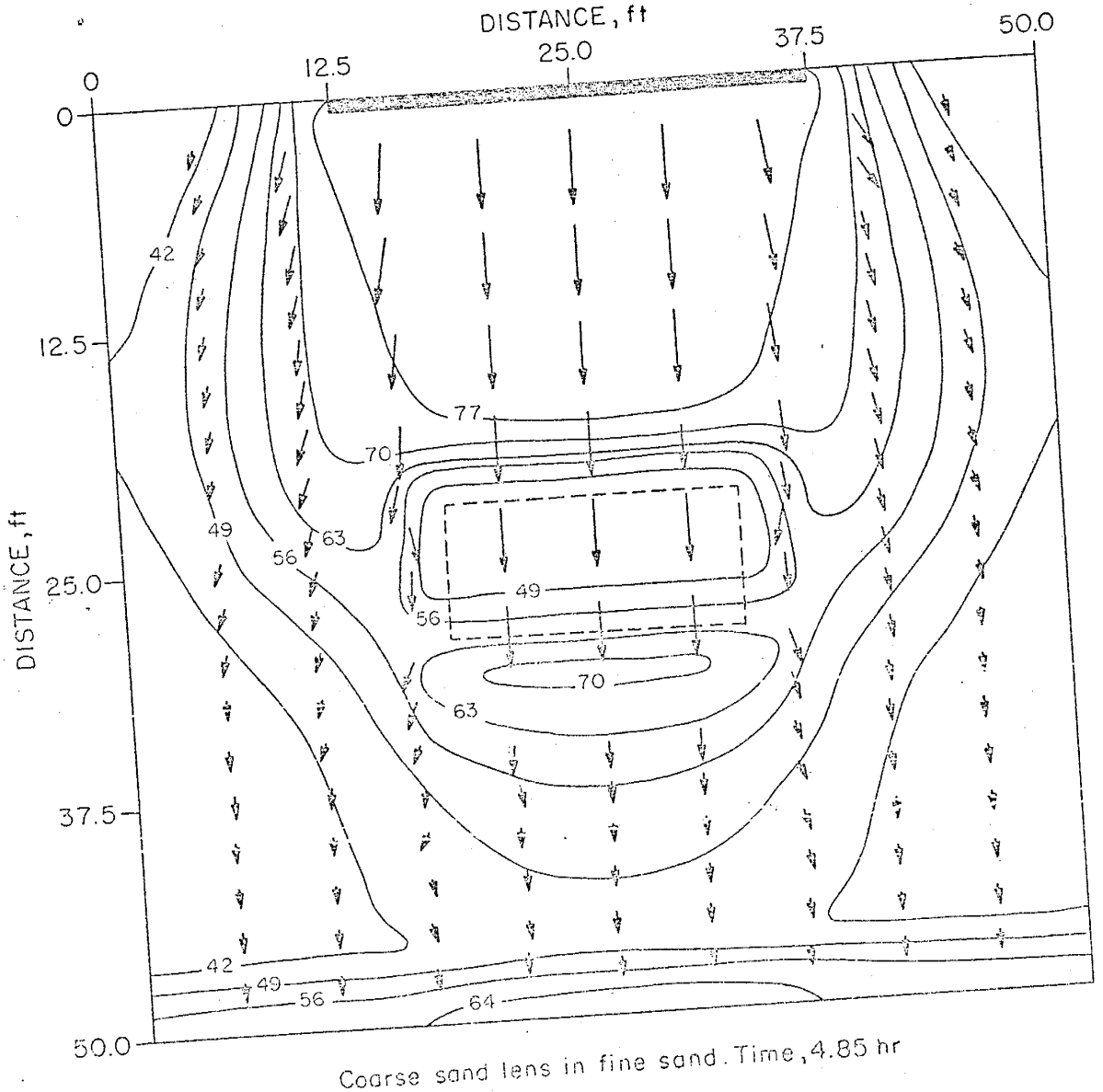
DISTANCE, ft
0
12.5
25.0
37.5
50.0
DISTANCE, ft
42
77
70
49
56
63
64
Coarse sand lens in fine sand. Time, 4.85 hr
EXPLANATION
Flux vector
1 inch ≈ 0.02 cm/sec
Leach pond
50
Saturation contour in percent saturation
Lens boundary

Figure 8

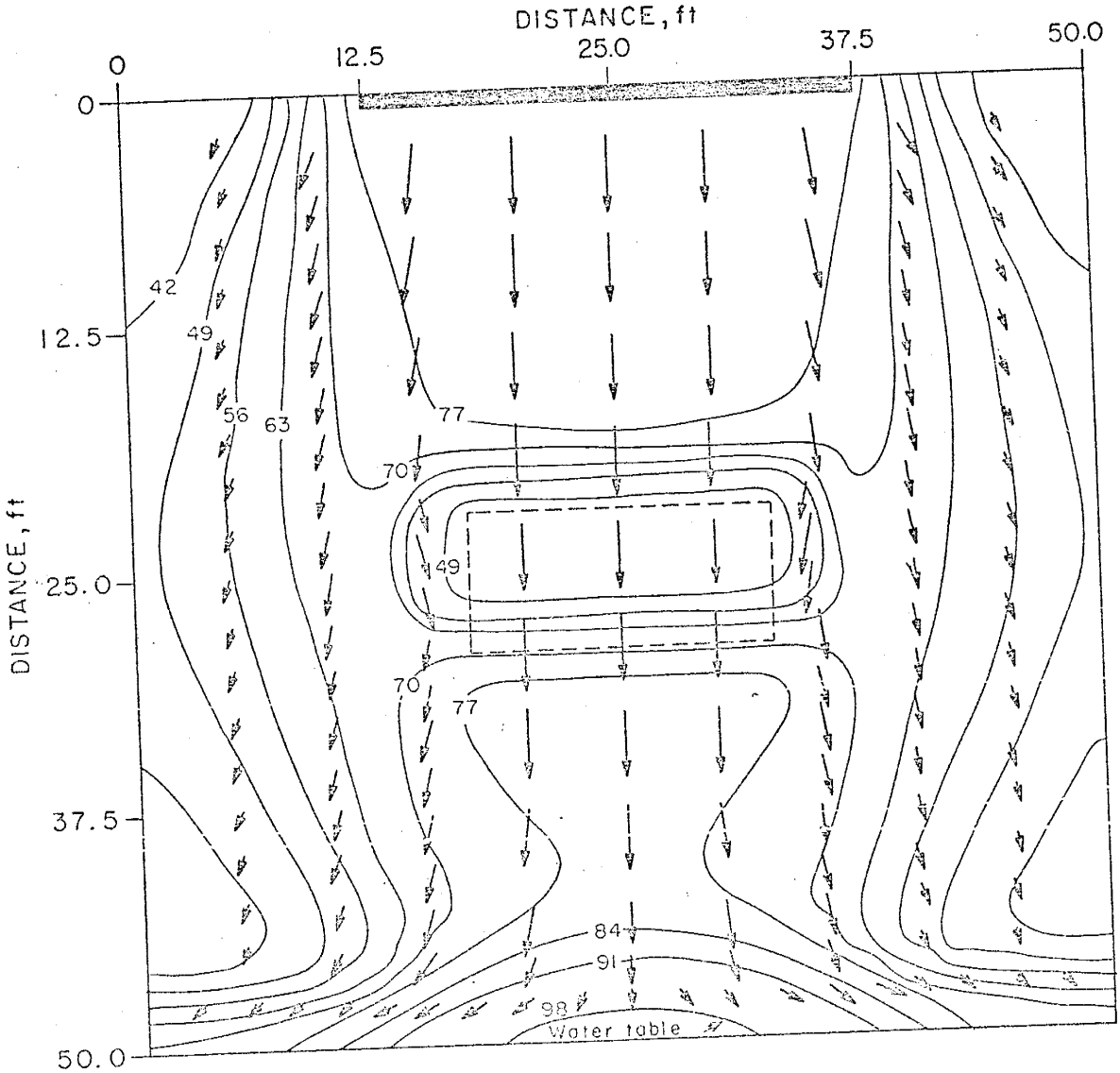

Coarse sand lens in fine sand .Time, 7.21 hr.

EXPLANATION

Flux vector
1 inch ≈ 0.02 cm/sec

Leach pond

50

Saturation contour in percent saturation

Lens boundary

Figure 9

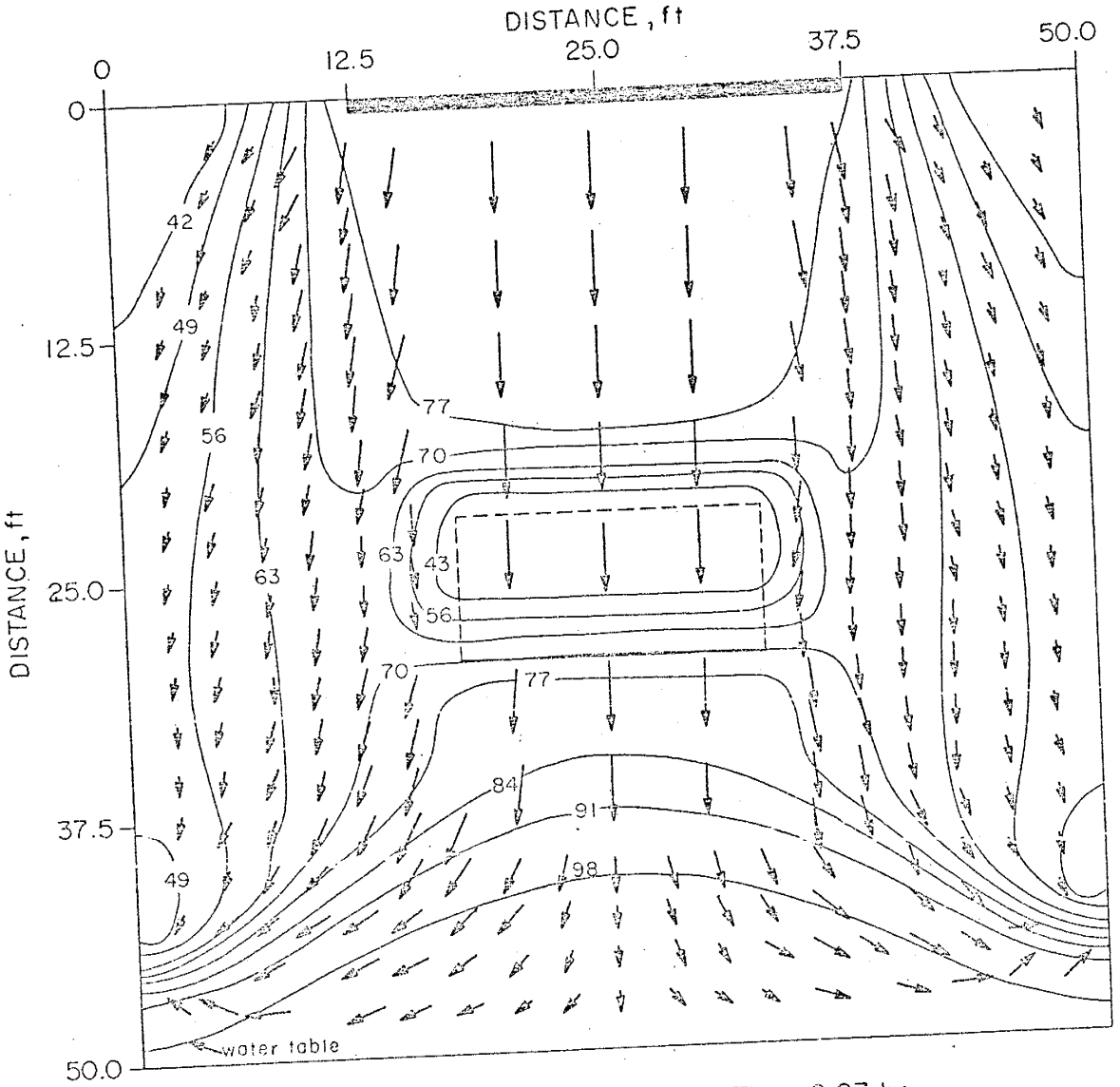

Coarse sand lens in fine sand. Time, 8.87 hr

EXPLANATION

Flux vector
1 inch ≈ 0.02 cm/sec

Leach pond

50 — Saturation contour in percent saturation

Lens boundary

Figure 10

water table mound is developing in the bottom of the flow domain, directly benaeth the center of the lens. This corresponds to the region of maximum flux vectors.

In Figure 10 we see that after 8.87 hours the water table mound has risen sharply compared to Case 1 after 9.67 hours. This is due to the channeling effect, whereby most of the solution is directed down a narrow flow avenue to the water table below.

The material balance at the end of this run was less than 0.6 percent total cumulative error. The computing time to develop the flow pattern of Figure 10 was about 30 minutes.

Case 3 Clay Lens in Fine Sand

Initial Hydrologic Properties:

A. Clay Lens

S_w = 40 %

S_{ri} = 30 %

ϕ = 20 %

k = 1 darcy

P_b = 120 cm

B. The fine sand surrounding the clay lens is the same as in Case 1.

Figures 11 through 13 show the effect that a semi-impermeable lens has on the flow pattern of Case 1. Leach dumps often have regions which remain dry and unleached. This situation is mainly due to layers of low permeability which prevent the flow of leach solution into the dry regions below.

We see in Figure 11 that after 4.38 hours that a perched water table has developed on the top of the clay lens situated in the center of the flow domain. Note also that the flux vectors near the perched water table indicate that the wetting front is being diverted away from the lens, furthermore, directly beneath the lens the flux vectors are very small, indicating virtually no flow in this region.

Figure 12 shows that after 9.51 hours the development of two small water table mounds at the bottom of the flow domain. The region directly beneath the clay lens is still a relatively dry region. We see that the perched water table has saturated the upper part of the clay lens.

In Figure 13 a water table trough has developed after 10.44 hours. The movement of the flux vectors is toward the dry region beneath the clay lens. The large or long flux vectors around the lens indicate that this is a region of maximum flow velocity relative to the rest of the flow domain. The possibility exists that due to these high flow rates that channels

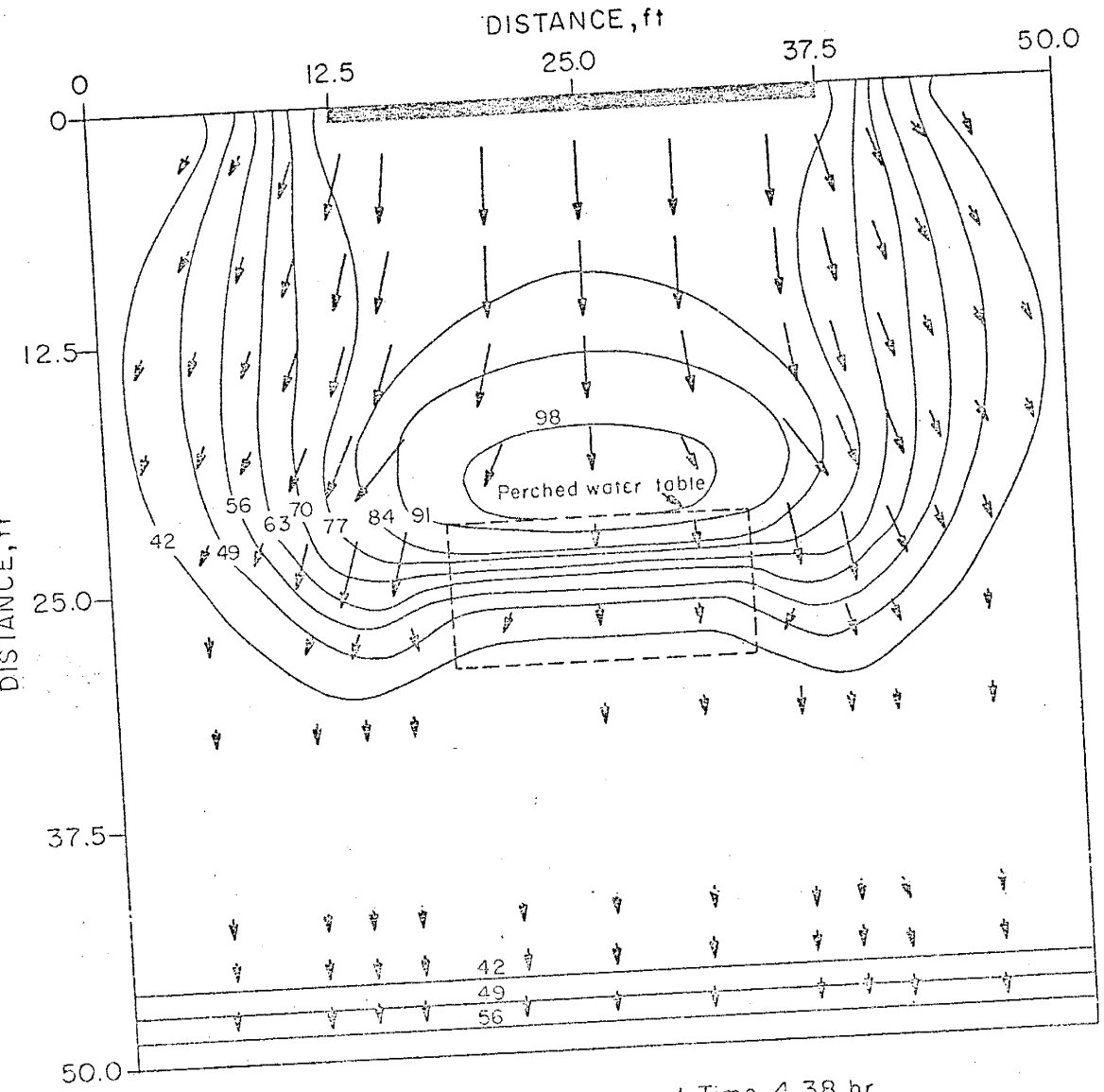

Clay lens in fine sand. Time, 4.38 hr.

EXPLANATION

Flux vector
1 inch ≈ 0.02 cm/sec

50 — Saturation contour in percent saturation

Leach pond

Lens boundary

Figure 11

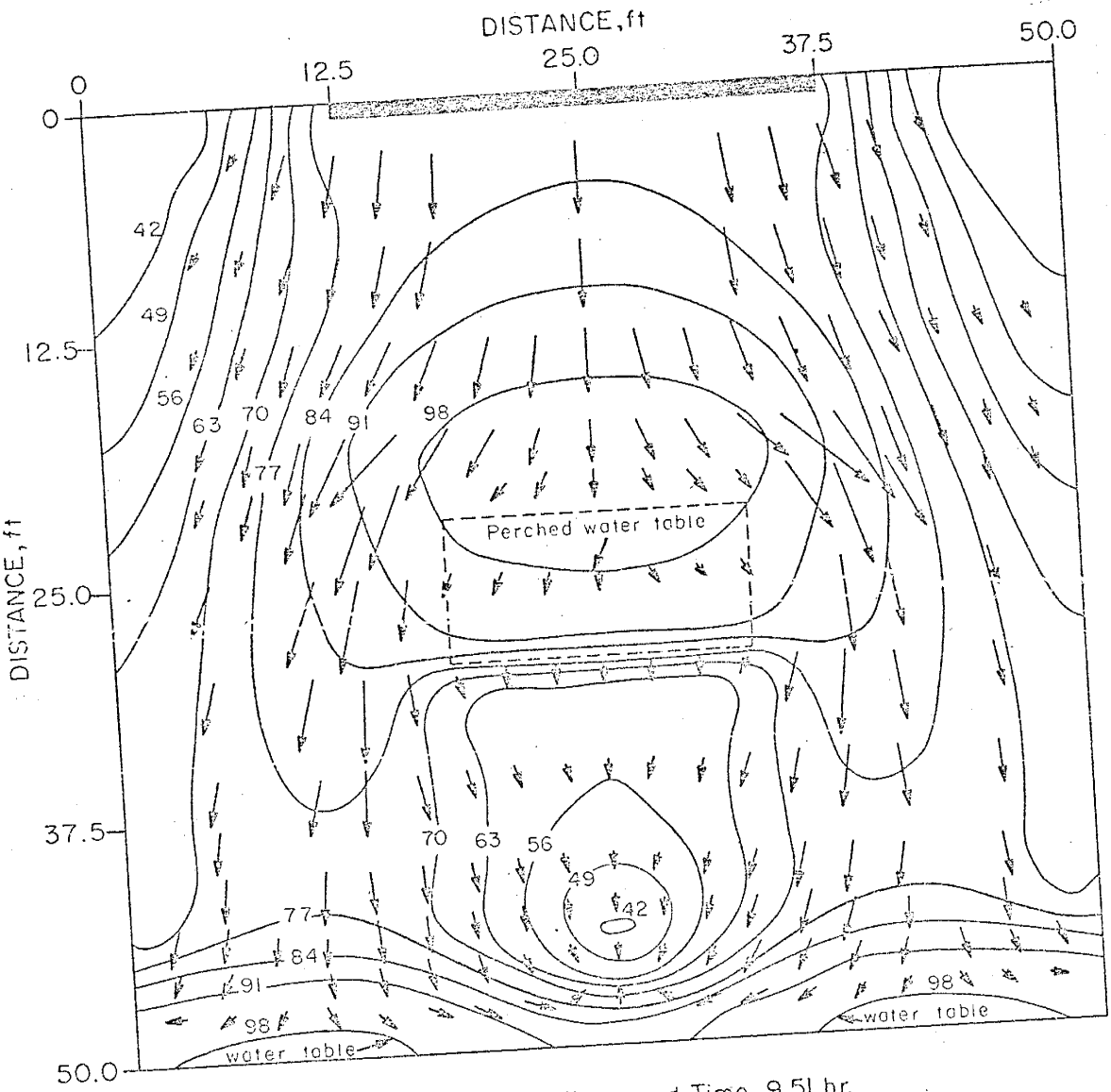

Clay lens in fine sand. Time, 9.51 hr.

EXPLANATION

Flux vector
1 inch ≈ 0.02 cm/sec

Leach pond

50 — Saturation contour in percent saturation

Lens boundary

Figure 12

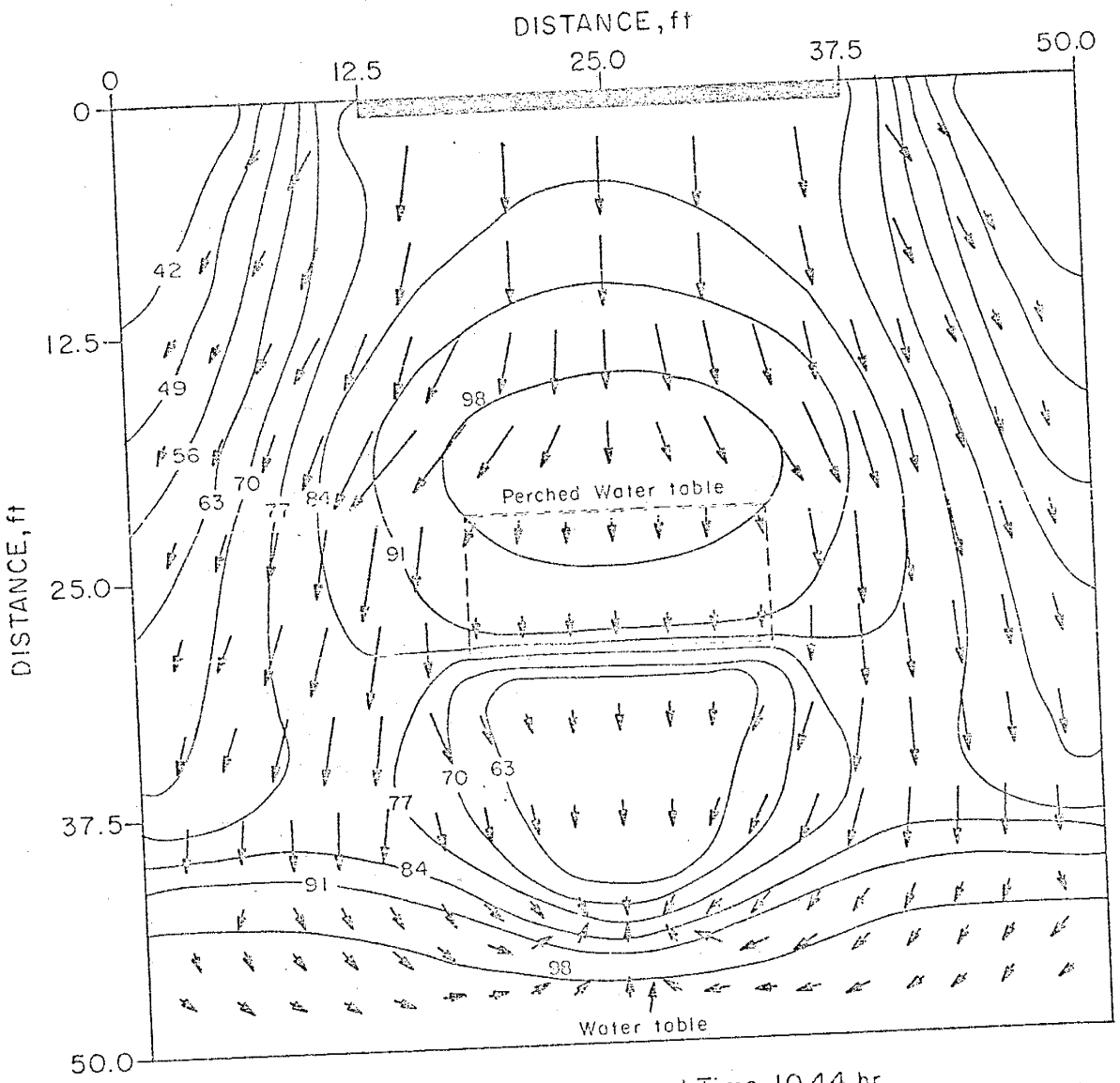

Clay lens in fine sand. Time, 10.44 hr.

EXPLANATION

Flux vector
1 inch ≈ 0.02 cm/sec

Leach pond

50 — Saturation contour in percent saturation

---------- Lens boundary

Figure 13

could develop. The total running time to simulate Figure 13 was approximatley 45 minutes.

Considering that in copper sulfide leach dumps the chemolithotrophic bacteria (see Bhappu, et al, 1969) need oxygen and carbon dioxide, it was noted that for all three cases modeled the saturation within the top 10 feet of the model leach dumps remained less that 85 % liquid saturation, indicates that for these cases the bacteria could probably live and multiply.

Hanson and Jacobson (a contribution to a USBM report on leach dumps, in preparation) found that the water table of an actural leach dump was not a smooth, flat surface, but had high and low anomalies. However, that study did not have information from enough well sites covering a large enough area to develop a detailed water table contour map. In particular, water table elevations were needed to delineate approximately the water table boundaries. From the three cases examined in this study it may be useful from the engineering standpoint, that channeling produces a steep water table and regions of low permeability, a water table trough. The possibility exists that a detailed water table map could be used to locate areas of very high and low permeability relative to most of the dump.

CONCLUSIONS

A numerical soultion was developed using a fully implicit finite differencing scheme for modeling two-dimensional, transient, unsaturated flow in a porous medium. Three cases of fluid flow in model leach dumps were simulated with the computer model developed in this study which produced symmetrical saturation contours and flux vectors throughout the flow domain. In all cases studied the computational time was relatively fast. Usually the number of iterations per time step were less than four and the material balance seldom exceeded one percent cumulative error.

In designing the computer model several new computational techniques were developed which are important since they together resulted in fast, stable simulations. One technique was the method of solving the solution matrix by alternating the direction of sweeping through the flow domain grid for successive iterations. This resulted in a very significant decrease (as much as 50 %) in the number of iterations per time step. Another technique was the coupling of the selection of a time step size with the size of the newly extrapolated dependent variables. Finally, the development of equation 7, and its derivative with respect to liquid saturation and capillary pressure head, was found to be very important to reducing the computational time when a water table developed in the simulation.

A new method is presented for estimating the hydraulic conductivity as a function of liquid saturation between grid cell boundaries.

The results of the simulation of cases 1,2 and 3 demonstrate that computer models of fluid flow in an unsaturated porous medium can play an important role in the engineering design and operation of future leach dumps. Further work in the computer model design to include dump consolidation and leaching chemistry will develop a very useful tool for leach dump engineers.

FUTURE WORK

The following plans are being formulated for extending this computer model and the results of this study:

1. Develop a procedure to model a seepage face which will rise with a rising water table.
2. Re-formulate the difference scheme and the definition of $K_{W_{av}}$ such that grid cells other than squares can be used.
3. Extend the model to three dimensions, both radial and Cartesian.
4. Introduce consolidation and leaching chemistry into the model in order to solve completely the problem of modeling a leach dump.
5. Develop analytical solutions as a means of discovering a better technique for averaging the hydraulic conductivities at grid cell boundaries for dynamic fluid flow.
6. Investigate more thoroughly the effective saturation equations presented in the section " Functional Relationships".

APPENDICES

APPENDIX A

Thomas Algorithm

The following development of the Thomas Algorithm was taken, with all of its criteria of limits, from von Rosenberg's (1969) presentation.

If the equation has the form

$$A_j \varphi^{n+1}_{i,j-1} + B_j \varphi^{n+1}_{i,j} + C_j \varphi^{n+1}_{i,j+1} = D_j \qquad \text{A-1}$$

between the limits used in the computer program of

$$2 \leq j \leq R-1 \qquad \text{(R is maximum outer limit)}$$

with $A_2 = C_R = 0$ (generally), then define a β_j and γ_j as

$$\beta_j = B_j - A_j C_{j-1} / \beta_{j-1} \qquad \text{A-2}$$

with $\beta_2 = B_2$ and

$$\gamma_j = (D_j - A_j \gamma_{j-1}) / \beta_j \qquad \text{A-3}$$

with

$$\gamma_2 = D_2 / B_2 \qquad \text{A-4}$$

The values of the dependent variables $\varphi^{n+1}_{i,j}$ are computed from

$$\varphi^{n+1}_{i,R} = \gamma_{R-1} \qquad \text{A-5}$$

and by a back calculation technique the new $\varphi^{n+1}_{i,j}$ are solved for by

$$\varphi^{n+1}_{i,j} = \gamma_j - C_j \varphi_{i,j+1} / \beta_j \qquad \text{A-6}$$

The Thomas algorithm is stable if $|B_j| \geq |A_j + C_j|$ for each equation of each grid cell of the flow domain.

APPENDIX B

Horizontal Sweep

The solution of the flow equations within each grid cell of the flow domain are solved alternately, first by moving the cross of Figure 2 vertically, in a vertical sweep, then on the next iteration, in a horizontal sweep, moving from left to right, from top to bottom. The equations used for the horizontal sweep are as follows:

$$A_i = K^{n+1}_{W_{i-1/2,j}} \qquad \text{B-1}$$

$$B_i = -(K^{n+1}_{W_{i+1/2,j}} + K^{n+1}_{W_{i-1/2,j}} + K^{n+1}_{W_{i,j+1/2}} + K^{n+1}_{W_{i,j+1/2}} + \Delta^2 \phi_{ij} E^{n+1/2}_{ij} / \Delta t^{n+1/2}) \qquad \text{B-2}$$

$$C_i = K^{n+1}_{W_{i+1/2,j}} \qquad \text{B-3}$$

$$D_i = -(\Delta^2 \phi_{ij} E^{n+1}_{ij} \varphi^{n}_{c\,ij} / \Delta t^{n+1/2} + \varphi^{n+1}_{c_{i+1,j}} K^{n+1}_{W_{i,j+1/2}} + \varphi^{n+1}_{c_{i,j-1}} K^{n}_{W_{i,j-1/2}}) \qquad \text{B-4}$$
$$+ \Delta^2 Q_{W_{ij}}$$

and

$$\varphi^{n+1}_{c_{i-1,j}} A_i + \varphi^{n+1}_{c\,ij} B_i + \varphi^{n+1}_{c_{i+1,j}} C_i = D_i \qquad \text{B-5}$$

APPENDIX C

Time Step Control Technique

A technique to control the size of the time step, in conjunction with an extrapolation technique (see Appendix D), is used in the computer model to increase computing speed and stability. This technique controls the size of a time step from the size of the last time step. If this maximum allowable time change produces an increase in the dependent variables over some preselected value, say a 10 per cent increase, then the routine selects a time step small enough to produce only that preselected increase in the dependent variables.

The routine also adjusts on the value of the dependent variable of the grid cell exhibiting the most change. In this manner the grid cells exhibiting the most change control the ultimate size of the time step for all cells within the flow domain.

The size of the time step is continuously being changed, usually it is being increased. But if drastic changes of the dependent variable do arise commensurate with the size of the last time step, the routire, in reducing the size of the time step to not exceed the desired limit on the change in the dependent variable, produces what appears to be a reduction in time step.

The overall effect of this routine over the simple method of a constant time step size is that at large time intervals there are fewer iterations, less machine roundoff error, and a more stable computer program.

APPENDIX D

Extrapolation Technique

The method of time step control is coupled to an extrapolation routine. From the maximum change in the dependent variables from the last time step, an estimate is made for a new set of φ's for the next time step.

This linear extrapolation (see Colgate and McKee, 1969) routine is based on the fact that the rate of change of the dependent variable from an old to a new time step is approximately the same, that is

$$\partial \varphi_c / \partial t_{old} \approx \partial \varphi_c / \partial t_{new} \qquad \text{D-1}$$

or

$$(\varphi_c^n - \varphi_c^{n-1}) / \Delta t^{n-1/2} = (\varphi_c^{n+1} - \varphi_c^n) / \Delta t^{n+1/2} \qquad \text{D-2}$$

Solving for φ_c^{n+1} gives the equation for selecting new starting values for $\varphi_{c_{new}}$:

$$\varphi_{c_{new}} = \Delta t^{n+1/2} / \Delta t^{n-1/2} (\varphi_c^n - \varphi_c^{n-1}) + \varphi_c^n \qquad \text{D-3}$$

APPENDIX E

Conductivities on Grids

In differencing equation 1 the hydraulic conductivities as a function of liquid saturation are defined at the boundary between grid cells (see Figure 2). The equation used to calculate the K_w's at the boundary between grid cells was derived by considering the physical aspects that both the saturated hydraulic conductivity and the conductivity as a function of liquid saturation have on the fluid flow. Equation 2 was used to define the hydraulic conductivity as a function of liquid saturation within a grid cell, that is,

$$K_w = K\, S_e^n \qquad 2$$

This equation, in terms of an average hydraulic conductivity as a function of liquid saturation at a grid cell boundary can be expressed as,

$$K_{w_{av}} = K_{av}\, S_{e_{av}}^n \qquad E\text{-}1$$

If the grid cells all have the same dimensions the above equation is written as,

$$K_{w_{av}} = (2K_1 K_2/(K_1 + K_2))((S_{e_1} + S_{e_2})/2)^n \qquad E\text{-}2$$

The harmonic mean is used to formulate the average value of the saturated hydraulic conductivities on the grid cell boundaries, thus resulting in a $K_{w_{av}}$

of zero if one of the grid cells has an absolute conductivity of zero. The effective saturations are averaged by the arithmetic mean, thus allowing fluid to flow into a grid cell if its hydraulic conductivity as a function of liquid saturation is zero but its saturated hydraulic conductivity is not zero.

APPENDIX F

Material Balance

The material balance is a method employed by the computer program, whereby a continuous check is made on the conservation of mass within a flow domain. The material balance used in this computer model calculates the cumulative volume of fluid being injected or removed by the source terms. The cumulative error is calculated as,

$$\% \text{ Cumulative error} = (V^n - V_k^n)100/V_k^n \qquad \text{F-1}$$

where

$$V_k^n = (\Sigma Q_{w_{ij}})(\text{Total elapsed time})\Delta^2 + (\Sigma S_{w_{ij}} \phi_{ij})\Delta^2_{(\text{initial})} \qquad \text{F-2}$$

$$V^n = (\Sigma S_{w_{ij}} \phi_{ij})\Delta^2 \qquad \text{F-3}$$

APPENDIX G

Stability Analysis

In order to show that the linearized form of equation 1 is unconditionally stable, the Fourier method of stability analysis developed by Von Neumann (see Richtmeyer and Morton, 1967) will be used to show that any roundoff error which developes in the numerical solution will not affect the desired approximation to the true result. The linearized form of equation 1 is,

$$K\,\partial^2\varphi_c/\partial x^2 + K\,\partial^2\varphi_c/\partial z^2 = E\partial\varphi_c/\partial t + Q_w \qquad G\text{-}1$$

The difference approximations are

$\Delta x = \Delta z$

$r = K\Delta t/\Delta x^2$

and

$$r(\varphi^{n+1}_{c_{i+1,j}} - 2\varphi^{n+1}_{c_{i,j}} + \varphi^{n+1}_{c_{i-1,j}} + \varphi^{n+1}_{c_{i,j+1}} - 2\varphi^{n+1}_{c_{ij}} + \varphi^{n+1}_{c_{i,j-1}}) =$$
$$E\,(\varphi^{n+1}_{c_{ij}} - \varphi^{n}_{c_{ij}}) + Q_{w_{ij}} \qquad G\text{-}2$$

It is assumed that no roundoff error develops in the constants Q_w, E and K. The difference equation, in the absence of roundoff error has an exact or true $\varphi^n_{c_{ij}}$(true). However, digital computers introduce roundoff error, therefore the actual computer solution $\varphi^n_{c_{ij}}$ will contain roundoff error e^n_{ij} and

$$\varphi^n_{c_{ij}} = \varphi^n_{c_{ij}}(\text{true}) + e^n_{ij} \qquad G\text{-}3$$

Substituting (G-3) into (G-2) yields

$$r\left(e^{n+1}_{i+1,j} - 2\, e^{n+1}_{i,j} + e^{n+1}_{i-1,j} + e^{n+1}_{i,j+1} - 2\, e^{n+1}_{i,j} + e^{n+1}_{i,j-1} \right) =$$
$$E\left(e^{n+1}_{i,j} - e^{n}_{i,j} \right) \qquad G\text{-}4$$

It will be assumed that periodic boundary conditions at the end points of the interval $0 \leq i \leq I$, $0 \leq j \leq J$ where $J\Delta x = I\Delta x = 2\pi$, and that the error can be expressed as a Fourier series as,

$$e^{n}_{i,j} = \lambda^{n}(k_x k_z \Delta t)\, \exp(\sqrt{-1}\,(k_x i \Delta x + k_z j \Delta z) \qquad G\text{-}5$$

Substituting the above Fourier form into equation (G-4) gives

$$E\,(\lambda^{n+1} - \lambda^{n})\, \exp(\sqrt{-1}\,(k_x i \Delta x + k_z j \Delta z) = \qquad G\text{-}6$$
$$-2r\lambda^{n+1} \exp(\sqrt{-1}\,(k_x i \Delta x + k_z j \Delta z)((1-\cos k_x \Delta x)+(1-\cos k_z \Delta z))$$

If the part containing the cosines is designated X, then the above equation reduces to

$$E\,(\lambda - 1) = -2r\,\lambda\,(X) \qquad G\text{-}7$$

or

$$E = (E + 2r(X))\lambda \qquad G\text{-}8$$

resulting in the form

$$\lambda = E/(E + 2rX) \qquad G\text{-}9$$

For stability $|\lambda| \leq 1$, which it is, since X is never negative in sign and $E \geq 0$.

APPENDIX H

Constant Head Boundary Condition

A constant head boundary condition can be introduced into the numerical solution. Equation 17 was written,

$$\varphi_{c_{i,j-1}} A_j + \varphi_{c_{ij}} B_j + \varphi_{c_{i,j+1}} C_j = D_j$$

To introduce a constant water level in a leach pond the following averaging process is used,

$$\frac{\varphi_{c_{i,2}} + \varphi_{c_{i,3}}}{2} = H \qquad \text{I-1}$$

where H is the 'head' of lixiviant in the leach pond.

Coupling equation 17 with (I-1) gives,

$$B_2 \varphi_{c_{i,2}} + C_2 \varphi_{c_{i,3}} = D_2 \qquad \text{I-2}$$

$$\varphi_{c_{i,2}} + \varphi_{c_{i,3}} = 2H$$

which results in defining the coefficients as

$B_2 = 1.0$

$C_2 = 1.0$

$D_2 = 2H$

$A_2 = 0.0$

For a water table at the bottom of the leach dump we have

$A_{j_{Max-1}} = 1.0$

$B_{j_{Max-1}} = 1.0$

$D_{j_{Max-1}} = 2H$

$C_{j_{Max-1}} = 0.0$

where j_{max} is the jth coordinate corresponding to the maximum depth of the model dump flow domain.

APPENDIX I

Computer Model

The computer program is presented in Fortran IV, in the form used to solve Case 1, the homogeneous fine sand. The program uses almost the same symbols used in the text when possible. For instance, the absolute hydraulic conductivity uses the symbol KO, the absolute permeability, KKO. The hydraulic conductivity as a function of fluid saturation is simply defined as K. The capillary pressure is PC, and the capillary potential heads are,

φ_c^n = PHI

φ_c^{n+1} = PHIA

Also,

S_w = S

S_e = SE

Arg2 = ARG

The other symbols used which may not be obvious to the reader are defined by "comment" statements within the following Fortran program.

```
C
C
C                    COMPUTER MODEL FOR UNSATURATED FLOW.....FORTRAN 4
C*****************************************************************************
C
C       MAIN
C
C       THE FOLLOWING COMMON BLOCK GOES BEFORE EACH SUBROUTINE
C
        IMPLICIT REAL*8(A-H,K,O-Z),INTEGER(I,J,L,M,N)
        COMMON K(22,22),PHI(22,22),PHIA(22,22),PHIK(22,22),PC(22,22),TIME,
       1S(22,22),OW(22,22),A(22),B(22),C(22),D(22),PB(22,22),VOLT,ERROR,
       2E(22,22),BETA(22),GAMA(22),POR(22,22),KO(22,22),SR(22,22),TSTOP,
       3TOL1,TOL2,FACTOR,Y1,Y2,Y3,Y4,AN,THETA,XTHETA,DT(2),DTIN,DTNPH,DEL,
       4DTNHH,JMAX,IMAX,NI,NJ,ITERAT,NED,NEDIT,JB,IB,M,VISL,DENL,GRV,TIMIN
       5,SE(22,22)
C
C       THE FOLLOWING COMMON STATMENT GOES BEFORE MAIN ONLY
C
        COMMON/PRINT/SSS,SSR,PPOR,KKO,PPB,I,J
C
C       READ IN DATA PERTINATE TO OPERATION OF MODEL
C
        READ(5,1)VISL,DENL,GRV
C        VIS=VISCOSITY,  DENL=DENSITY LIQUID,  GRV=GRAVITATIONAL CONSTANT
        READ(5,2)TSTOP
C        TSTOP=TOTAL  TIME TO BE MODELLED BY PROGRAM
        READ(5,3)DEL,DTIN,TIMIN,FACTOR,TOL2,TOL1
C        DEL=GRID LENGTH,  DTIN=INITIAL STARTING TIME IN SECONDS
C        TIMIN=TIME STEP INCREMENT
C        TOL2=MAXIMUM ALLOWABLE ITERATION PER TIME STEP
C        TOL1=CONVERGENCE CRITERIA
        READ(5,4)IMAX,JMAX
C IMAX=MAXIMUM NUMBER OF GRIDS INCLUDING DUMMY GRIDS, IN X DIRECTION
C JMAX=MAXIMUM NUMBER OF GRIDS INCLUDING DUMMY GRIDS, IN Z DIRECTION
        READ(5,6)NED
C       NED IS A COUNTER EQUAL TO A NUMBER OF TIME STEPS BETWEEN PRINTOUT
C        FACTOR IS THE DESIRED MAXIMUM CHANGE IN HEAD PER TIME STEP
        READ(5,9)AN
C        AN=PERCENT ANISOTROPY
C
C       FORMAT
C
    1 FORMAT(2F10.8,F10.5)
    2 FORMAT(D10.4)
    3 FORMAT(5F10.5,F18.15)
    4 FORMAT(2I2)
    5 FORMAT(5F10.5)
    6 FORMAT(I3)
    9 FORMAT(F10.5)
C
C
C       ALFA AND BET ARE THE ALFA AND BETA CONSTANTS.
C       FOR GENERAL PROBLEMS THE FOLLOWING VALUES WILL SUFFICE
C       AND ARE THEREFORE NOT INCLUDED IN THE COMMON BLOCK
C
        ALFA=1.56
        BET=0.4
C
        CALL PRINT1
C
        IB=IMAX-1
        JB=JMAX-1
C
C       READ IN INITIAL FIELD DATA FOR EACH LAYER FROM TOP TO BOTTOM
C
        DO 1000 J=2,JB
        READ(5,5)SSS,SSR,PPOR,KKO,PPB
        DO 1000 I=2,IB
        S(I,J)=SSS
        SR(I,J)=SSR
        PB(I,J)=PPB
        POR(I,J)=PPOR
        KO(I,J)=KKO*.9870-08*DENL*GRV/VISL
        PC(I,J)=ALFA*PB(I,J)+BET*PB(I,J)*DLOG((1.-S(I,J))/(S(I,J)-SSR))
        PHI(I,J)=PC(I,J)+DEL*(J-1.5)
        PHIA(I,J)=PHI(I,J)
        CALL PRINT2
 1000 CONTINUE
C
C       SET INITIAL TIME
C
        TIME=.0
C
        NEDIT=0
C
        DTNHH=DTIN
        DTNPH=DTNHH
        Y1=0.0
        Y4=0.0
C
C       SET BOUNDARY CONDITIONS
C
        DO 66 J=2,JB
        KO(1,J)=0.0
        KO(IMAX,J)=0.0
        SE(1,J)=0.0
        SE(IMAX,J)=0.0
   66 CONTINUE
        DO 67 I=1,IMAX
        KO(I,1)=0.0
        KO(I,JMAX)=0.0
        SE(I,1)=0.0
        SE(I,JMAX)=0.0
   67 CONTINUE
C
        DO 11 J=2,JB
        DO 11 I=2,IB
        OW(I,J)=0.0
   11 CONTINUE
C
C       CALCULATE INITIAL AMOUNT OF LIQUID IN SYSTEM
C
        Y2=0.0
        DO 12 J=2,JB
        DO 12 I=2,IB
        Y2=S(I,J)*POR(I,J)+Y2
   12 CONTINUE
        Y2=Y2*DEL*DEL
C
        CALL CENTER
        STOP
        END
```

```
C*************************************************************************
C
C
      SUBROUTINE CENTER
C
C     CENTER IS THE MAIN CONTROL SUBROUTINE
C
      BET=0.4
      ALFA=1.56
C
    1 CALL DELTIM
      ITERAT=1
      CALL XTRAP
      ODES=1.0-04
      OW(9,2)=ODES
  100 CALL VSWEEP
      IT=1
      GO TO 99
C
  110 CALL RSWEEP
      IT=2
C
C     CHECK TOLERANCE
C
   99 PKMAX=0.0
      DO 4 J=2,JB
      DO 4 I=2,IB
      PBD=.01
      SS=DABS(PHIK(I,J)-DEL*(J-1.5))+PBD
      PPK=DABS((SSA-SS)/SSA)
      SSA=DABS(PHIA(I,J)-DEL*(J-1.5))+PBD
      IF(PPK-PKMAX)4,3,3
    3 PKMAX=PPK
      NI=I
      NJ=J
    4 CONTINUE
      IF(PKMAX.LE.TOL1)GO TO 8
      ITERAT=ITERAT+1
      IF(ITERAT.GT.TOL2)GO TO 8
C
C     SET FUNCTIONAL RELATIONSHIPS FOR K TH ITERATE
C
      DO 5 J=2,JB
      DO 5 I=2,IB
      PHIK(I,J)=PHIA(I,J)
      PC(I,J)=PHIA(I,J)-DEL*(J-1.5)
      ARG=(PC(I,J)-ALFA*PP(I,J))/(BET*PB(I,J))
      IF(ARG.GE.30.)ARG=30.
      IF(ARG.LT.-30.)ARG=-30.
      EARG=DEXP(ARG)
      OPEARG=1.+EARG
      OMSR=1.-SR(I,J)
      ZIP=1./(OPEARG*OPEARG*BET*PB(I,J))
      ZAP=EARG*OMSR
      E(I,J)=ZIP*ZAP
      SE(I,J)=1./OPEARG
    5 CONTINUE
C
C
      IF(IT.EQ.1)GO TO 110
      IF(IT.EQ.2)GO TO 100
C
C     EVALUATE FUNCTIONAL RELATIONSHIPS AFTER ITERATION
C
    8 DO 9 J=2,JB
      DO 9 I=2,IB
      PC(I,J)=PHIA(I,J)-DEL*(J-1.5)
      ARG=(PC(I,J)-ALFA*PP(I,J))/(BET*PB(I,J))
      IF(ARG.GE.30.)ARG=30.
      IF(ARG.LT.-30.)ARG=-30.
      EARG=DEXP(ARG)
      OPEARG=1.+EARG
      OMSR=1.-SR(I,J)
      ZIP=1./(OPEARG*OPEARG*BET*PB(I,J))
      ZAP=EARG*OMSR
      E(I,J)=ZIP*ZAP
      SE(I,J)=1./OPEARG
      S(I,J)=OMSR/OPEARG+SR(I,J)
      K(I,J)=KO(I,J)*SE(I,J)*SE(I,J)
    9 CONTINUE
C
C      ENTER ANY VARIABLE SOURCE OR SINK TERMS HERE
C
C
C     INTERCHANGE ARRAYS OF OLD AND NEW HEAD VALUES
C
      DO 500 I=2,IB
      DO 500 J=2,JB
      TEMP=PHI(I,J)
      PHI(I,J)=PHIA(I,J)
      PHIA(I,J)=TEMP
  500 CONTINUE
C
C      UPDATE MAT. BALANCE
C
      CALL MATBAL
C
C      CHECK TIME ELAPSED
C
      NEDIT=NEDIT+1
      IF((TIME-TSTOP).GE.0.0)GO TO 12
      IF(NEDIT.LT.5)GO TO 77
      IF((NEDIT-NEDIT/NED*NED).NE.0)GO TO 1
C
   77 CALL RESULT
      GO TO 1
   12 CONTINUE
C
      CALL MATBAL
C
      CALL RESULT
      RETURN
      END
```

```
C*****************************************************************************
C
C     SUBROUTINE DELTIM
C     THIS ROUTINE CONTROLS MAXIMUM VARIATION IN HEADS PER TIME STEP
C     DTNMH=DTNPH
C      INCREMENT TIME STEP WITH TIMIN (TIME INCREASE)
C     DT(1)=TIMIN*DTNMH
      DMAX=0.0
C     COMPARE MAGNITUDE OF HEAD CHANGE BETWEEN ZONES PER TIME STEP
      DO 1 J=2,JB
      DO 1 I=2,IB
C      PERFORM PROCEEDURE TO CROSS WATER TABLE.
      PBD=PB(I,J)*.5
      PC1=ABS(PHIA(I,J)-DEL*(J-1.5))+PBD
      PC2=ABS(PHI(I,J)-DEL*(J-1.5))+PBD
      DDD=ABS((PC1-PC2)/PC1)
C     IF((DDD-DMAX).LE.0.0)GO TO 1
      DMAX=DDD
    1 CONTINUE
      IF(DMAX.LE.0.0)GO TO 2
      FACT=FACTOR/DMAX
      DT(2)=DTNMH*FACT
      GO TO 3
    2 DT(2)=1.D+20
    3 CONTINUE
      DTMIN=1.D+40
C     CHECK IF MAX VARIATION GREATER THAN FACTOR
      DO 4 I=1,2
      IF((DTMIN-DT(I)).LE.0.0)GO TO 4
      DTMIN=DT(I)
    4 CONTINUE
      DTNPH=DTMIN
      TIME=TIME+DTNPH
      RETURN
      END
C*****************************************************************************
C
C     SUBROUTINE XTRAP
C     SUBROUTINE FOR EXTRAPOLATION OF NEW HEADS FOR A NEW TIME STEP
C
      ALFA=1.56
      BET=0.4
      RDT=DTNPH/DTNMH
C      EXTRAPOLATE NEW VALUES OF HEAD
C
      DO 3 J=2,JB
      DO 3 I=2,IB
      PHIA(I,J)=PHI(I,J)+RDT*(PHI(I,J)-PHIA(I,J))
      PHI(I,J)=PHIA(I,J)
      PC(I,J)=PHIA(I,J)-DEL*(J-1.5)
      ARG=(PC(I,J)-ALFA*PB(I,J))/(BET*PB(I,J))
      IF(ARG.GE.30.)ARG=30.
      IF(ARG.LT.-30.)ARG=-30.
      EARG=DEXP(ARG)
      OPEARG=1.+EARG
      OMSR=1.-SR(I,J)
      ZIP=1./(OPEARG+OPEARG*BET*PB(I,J))
      ZAP=EARG*OMSR
      E(I,J)=ZIP*ZAP
      SE(I,J)=1./OPEARG
    3 CONTINUE
      RETURN
      END
C*****************************************************************************
C
C     SUBROUTINE MATBAL
C     MATERIAL BALANCE ON SATURATION OR WATER CONTENT
C
C      TOTAL ALL SOURCE AND SINKS
C
      Q=0.0
      DO 22 J=2,JB
      DO 22 I=2,IB
      Q=Q+P(I,J)+Q
   22 CONTINUE
C     VKSUBN=Q*TIME*DEL*DEL+Y2
C
      SUMS=0.0
      DO 2 J=2,JB
      DO 2 I=2,IB
      SUMS=S(I,J)*POR(I,J)+SUMS
    2 CONTINUE
C     VSUBN=SUMS*DEL*DEL
C
C     IF(VKSUBN.EQ.0.0)GOTO 3
C
C     ERROR=(VSUBN-VKSUBN)*100./VKSUBN
C
C     GO TO 4
    3 IF(TSUMS.EQ.0.0)GO TO 4
      ERROR=SUMS/TSUMS
    4 TSUMS=SUMS
      Y1=Y1+Q*TIME*DEL*DEL
      RETURN
      END
```

```
C*****************************************************************************
C
C
C     SUBROUTINE VSWEEP
C
C     SOLUTION OF THOMAS ALGORITHM BY LINE SWEEP IN VERTICAL DIRECTION
C
C
C     SET A,B,C,AND D COEFFICIENTS OF THOMAS ALGORITHM
C
      DO 200 I=2,IB
      DO 100 J=2,JB
      KR=    KO(I,J)*KO(I+1,J)/(KO(I,J)+KO(I+1,J))*
     $     ((SE(I,J)+SE(I+1,J))*(SE(I,J)+SE(I+1,J)))*.5
      KL=    KO(I,J)*KO(I-1,J)/(KO(I,J)+KO(I-1,J))*
     $     ((SE(I,J)+SE(I-1,J))*(SE(I,J)+SE(I-1,J)))*.5
      KU=    KO(I,J)*KO(I,J-1)/(KO(I,J)+KO(I,J-1))*
     $     ((SE(I,J)+SE(I,J-1))*(SE(I,J)+SE(I,J-1)))*.5
      KD=    KO(I,J)*KO(I,J+1)/(KO(I,J)+KO(I,J+1))*
     $     ((SE(I,J)+SE(I,J+1))*(SE(I,J)+SE(I,J+1)))*.5
      A(J)=KU
      B(J)=-(KL+KR+KU+KD+DEL*DEL*POR(I,J)*E(I,J)/DTNPH)
      C(J)=KD
      D(J)=-(DEL*DEL*POR(I,J)*E(I,J)*PHI(I,J)/DTNPH+PHIK(I+1,J)*KR+
     1PHIA(I-1,J)*KL)+DEL*DEL*QW(I,J)
  100 CONTINUE
C
C     SET BETA AND GAMMA COEFFICIENTS OF THOMAS ALGORITHM
C
C
C     ANY HEAD CONDITION CHANGES ARE ENTERED IN HERE
C
C
      GAMA(2)=D(2)/B(2)
      BETA(2)=B(2)
      DO 101 J=3,JB
      BETA(J)=B(J)-A(J)*C(J-1)/BETA(J-1)
      GAMA(J)=(D(J)-A(J)*GAMA(J-1))/BETA(J)
  101 CONTINUE
C
C     SET THE JMAX OR BOTTOM BOUNDARY VALUE FOR THE NEW HEAD
C
      PHIA(I,JB)=(D(JB)-A(JB)*GAMA(JB-1))/BETA(JB)
C
C     PERFORM BACK CALCULATION OF HEADS
C
      JC=JB-2
      DO 200 JJ=1,JC
      M=JB-JJ
      PHIA(I,M)=GAMA(M)-C(M)*PHIA(I,M+1)/BETA(M)
  200 CONTINUE
      RETURN
      END
C*****************************************************************************
C
C
      SUBROUTINE RSWEEP
C
C      SOLUTION OF THOMAS ALGORITHM BY LINE SWEEP FROM LEFT TO RIGHT
C
C
C     SET A,B,C,AND D COEFFICIENTS OF THOMAS ALGORITHM
C
      JJB=JB-1
      DO 200 J=2,JB
      DO 100 I=2,IB
      KR=    KO(I,J)*KO(I+1,J)/(KO(I,J)+KO(I+1,J))*
     $     ((SE(I,J)+SE(I+1,J))*(SE(I,J)+SE(I+1,J)))*.5
      KL=    KO(I,J)*KO(I-1,J)/(KO(I,J)+KO(I-1,J))*
     $     ((SE(I,J)+SE(I-1,J))*(SE(I,J)+SE(I-1,J)))*.5
      KU=    KO(I,J)*KO(I,J-1)/(KO(I,J)+KO(I,J-1))*
     $     ((SE(I,J)+SE(I,J-1))*(SE(I,J)+SE(I,J-1)))*.5
      KD=    KO(I,J)*KO(I,J+1)/(KO(I,J)+KO(I,J+1))*
     $     ((SE(I,J)+SE(I,J+1))*(SE(I,J)+SE(I,J+1)))*.5
      A(I)=KL
      B(I)=-(KL+KR+KU+KD+DEL*DEL*POR(I,J)*E(I,J)/DTNPH)
      C(I)=KR
      D(I)=-(DEL*DEL*POR(I,J)*E(I,J)*PHI(I,J)/DTNPH+PHIK(I,J+1)*KD+
     1PHIA(I,J-1)*KU)+DEL*DEL*QW(I,J)
  100 CONTINUE
C
C     SET BETA AND GAMMA COEFFICIENTS OF THOMAS ALGORITHM
C
      BETA(2)=B(2)
      GAMA(2)=D(2)/B(2)
      DO 101 I=3,IB
      BETA(I)=B(I)-A(I)*C(I-1)/BETA(I-1)
      GAMA(I)=(D(I)-A(I)*GAMA(I-1))/BETA(I)
  101 CONTINUE
C
C      SET THE OUTER (IB) BOUNDARY VALUES OF HEAD
C
      PHIA(IB,J)=(D(IB)-A(IB)* GAMA(IB-1))/ BETA(IB)
C
C     PERFORM BACK CALCULATION OF HEADS
C
      IC=IB-2
      DO 200 II=1,IC
      M=IB-II
      PHIA(M,J)= GAMA(M)-C(M)*PHIA(M+1,J)/ BETA(M)
  200 CONTINUE
      RETURN
      END
C*****************************************************************************
C
C
C     SUBROUTINE RESULT PRINTS OUT RESULTS OF CALCULATIONS
C     SUBROUTINE PRINT1 PRINTS OUT INFORMATION PERTINATE TO MODEL ONLY
C     SUBROUTINE PRINT2 PRINTS OUT INFORMATION ON FIELD DATA PER LAYER
```

REFERENCES CITED

Ames, W. F. (1965), Nonlinear Partial Differential Equations in Engineering, Academic Press, New York.

Anon, (1966), Cu Metal Formula; Rip and Leach, Engineering and Mining Journal, 167, 84-85.

Ballard, J. K. (1971), Solution Mining, Mining Engineer, 23, 109.

Breitenbach, E. A., D. H. Thurnau, H. K. van Poolen, (1968)

(a) Immiscible Fluid Flow Simulator, SPE 2019,

(b) The Fluid Flow Simulation Equations, SPE 2020,

(c) Solution of the Immiscible Fluid Flow Simulation Equations, SPE 2021,

(d) Treatment of Individual Well and Grids in Reservoir Modeling, SPE 2022, papers presented at the symposium on Numerical Simulation of Reservoir Performance.

Brooks, R. H., A. T. Corey, (1964), Hydraulic Properties of Porous Media, Hydrology Papers, No. 3, Colo. State Univ., Fort Collins, Colo.

Brutsaert, W., (1966), Probability Laws for Pore-Size Distributions, Soil Science, 101, 85-92.

Carslaw, H. S., J. C. Jaeger, (1959), Conduction of Heat in Solids, 2nd. edition, Oxford at the Clarendon Press, New York.

Coats, K. H., R. L. Nielsen, M. H. Terhune, A. G. Weber, (1967), Simulation of Three-Dimensional, Two-Phase Flow in Oil and Gas Reservoirs, Petroleum Engineers Journal, Dec., 377-388.

Colgate, S. A., C. McKee, Early Supernova Luminosity,(1969) The Astrophysical Journal, 157, 623-643.

Freeze, R. A.,(1971), Three-Dimensional, Transient, Saturated-Unsaturated Flow in a Groundwater Basin, Water Resources Research, 7, 347-366.

Freeze, R. A., (1969), The Mechanism of Natural Ground Water Recharge and Discharge 1. One-Dimensional, Vertical, Unsteady, Unsaturated Flow Above a Recharging or Discharging Ground Water Flow System, Water Resources Research, 5,153-171.

Hardwick, W. R., (1967), Fracturing a Deposit with with Nuclear Explosives and Recovering Copper by the In-Situ Leaching Method, United States Bureau of Mines Report of Investigation 6926.

Harris, J. A., (1969), Development of a Theoretical Approach to the Heap Leaching of Copper Sulfide Ores, Proceedings of the Australian Institute of Mining and Metallurgy, 230, 81-92.

Howard, E. V., (1968), Chino Uses Radiation Logging for Studying Dump Leaching Process, Mining Engineering, Apr., 70-74.

Jeppson, R. W., (1970), Transient Flow of Water From Infiltrometers-Formulation of Math. Model and Preliminary Numerical Solutions and Analysis of Results, PRWG-59c-2, Utah State Univ., Logan, Utah.

Kealy, C. D., R. E. Williams, (1971), Flow through a Tailings-Pond Embankment, AIME preprint No. 71-AC-33.

Liakopoulos, A. C., (1963), Transient Flow Through Unsaturated Porous Media, A dissertation, Univ. California at Berkeley.

Malouf, E. E., (1970), Bicentrastive Mining, A short course, AIME Annual Meeting, Feb.

Peaceman, D. W., (1967), Chapter 10, A Symposium on Methods of Solution, W. F. Ames, editor, Academic Press, New York.

Richards, L. A., (1931), Capillary Conduction of Liquids Through Porous Mediums, Physics, 1, 318-333.

Richtmeyer, R. D., K. W. Morton, (1967), Difference Methods for Initial-Value Problems, 2nd. edition, John Wiley and Sons, Inc., New York.

Rubin, J., (1968), Theoretical Analysis of Two-Dimensional Transient Flow of Water in Unsaturated and Partly Unsaturated Soils, Proceedings of the Soil Science Society of America, 32, 607-615.

Sheffer, H. W., L. G. Evens, (1968), Copper Leaching in the Western United States, United States Bureau of Mines Information Circular No. 8341.

von Rosenberg, D. U., (1969), Methods for Numerical Solution of Partial Differential Equations, American Elsevier Publishing Co., Inc., New York.

Weiss, A., (1969), A Decade of Digital Computing in the Mineral Industry, Society of Mining and Metallurgical Engineers Activity Fund of the AIME, New York.

Woodcock, J. J., (1967), Copper Waste Dump Leaching, Proceedings of the Australian Institute of Mining and Metallurgy, 224, 47-66.

This thesis is accepted on behalf of the faculty of the Institute by the following committee:

Ronald F. Roman

Gerardo Wolfgang Gyssens

Mark E. Swanson

Willem Brutsaert

Ralph M. McGehee

Date Aug 2, 1971